

EXPERIMENTAL AND NUMERICAL ANALYSIS
OF STRESSES AROUND UNREINFORCED
AND REINFORCED WEB OPENINGS

by

JAMES CHEN-MING HUANG

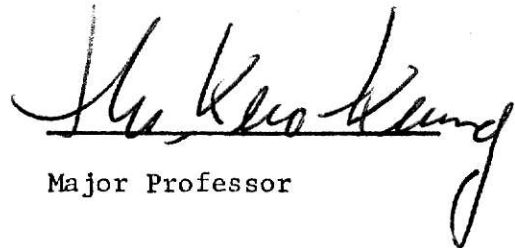
DIPLOMA, TAIPEI INSTITUTE OF TECHNOLOGY, 1969

A MASTER'S THESIS
submitted in partial fulfillment of the
requirements for the degree

MASTER OF SCIENCE
Department of Civil Engineering
KANSAS STATE UNIVERSITY
Manhattan, Kansas

1976

Approved by:



Major Professor

LD
2068
T4
1976
H83
e 2

TABLE OF CONTENTS

Document	Page
LIST OF FIGURES	iii
LIST OF TABLES	v
LIST OF SYMBOLS	vi
I. INTRODUCTION	1
II. LITERATURE SURVEY	5
III. METHODS OF ANALYSIS	
A. LEAST WORK METHOD	8
B. VIERENDEEL METHOD	16
IV. EXPERIMENTAL STUDIES	
A. BRITTLE-COATING METHOD	18
B. ELECTRICAL RESISTANCE STRAIN GAGE METHOD	26
V. COMPARISON AND DISCUSSION OF RESULTS	33
VI. CONCLUSIONS	37
APPENDICES	38
REFERENCES	48
ACKNOWLEDGEMENTS	50

LIST OF FIGURES

Figure		Page
1.	Simply Supported Beam	3
2.	Web Opening and Reinforcing Details	3
3.	Beam Cross Section Details	4
4.	Two Loading Types	4
5.	A Partition of Ring Structure	8
6.	Division of Ring Structure into Curved Beam and Straight Beam Segments	9
7.	Cross Section of Curved Beam	10
8.	Freebody Diagram of a Curved Beam	14
9.	Freebody Diagram for Vierendeel Analysis	16
10.	Threshold Strain Vs. Coating Thickness	21
11.	Loading Vs. Time in Brittle-Coating Tests	22
12.	Photographs of Stress-Coating Crack Pattern and Contour Lines	23
13.	Stress-Coating Contour Lines at Unreinforced Corner	24
14.	Stress-Coating Contour Lines at Reinforced Corner	25
15.	Strain Gage Locations and Rosette Details	27
16.	Typical Strain-Loading Diagram of Strain Gage Measurements	29
17.	Normal Stress Distribution Curves by Brittle- Coating Method	34

LIST OF FIGURES (Cont.)

Figure		Page
18.	Normal Stress Curves for Unreinforced Opening by Electrical Resistance Strain Gage Method	35
19.	Normal Stress Curves for Reinforced Opening by Electrical Resistance Strain Gage Method	36
A.	Freebody Diagram for Loading Case I	38
B.	Dimensions of Section A-A	39
C.	Typical Section	40
D.	Normal Stress Curve for Section A-A	40
E.	Freebody Diagram for Section B-B	40
F.	Normal Stress Curve for Section B-B	41
G.	A Freebody Diagram for Section D-D	41
H.	Dimensions of Section D-D	42
K.	Normal Stress Curve for Section D-D	43
L.	Freebody Diagram for Section C-C	43
Q.	Normal Stress Curve for Section C-C	43
R.	Normal Stress Curve for Unreinforced Corner by Brittle-Coating Method	46
S.	Normal Stress Curve for Reinforced Corner by Brittle-Coating Method	47

**THIS BOOK
CONTAINS
NUMEROUS PAGES
WITH ILLEGIBLE
PAGE NUMBERS
THAT ARE CUT OFF,
MISSING OR OF POOR
QUALITY TEXT.**

**THIS IS AS RECEIVED
FROM THE
CUSTOMER.**

LIST OF TABLES

Table	Page
1. Brittle-Coating Calibration Bar Test Record	19
2. Corrected Strain Gage Readings for Loading Case I	30
3. Corrected Strain Gage Readings for Loading Case II	31
4. Results of Rosette Analysis	32
5. A Comparison List of Critical Normal Stresses	32
A. Computation of Effective Width and Section Properties	42
B. A Record of Brittle Coating Test	44
C. Threshold Strain Correction Due to Temperature and R.H.	45
D. Computation of Apparent Stress by Brittle-Coating Method	46

LIST OF SYMBOLS

A	area of a section
b	width of flange or horizontal dimension at point of interest
b'	transformed width of flange
E	Young's Modulus (use 29×10^6 psi for steel)
I	second moment of inertia of a section with respect to its centriodal axis
I_n	n^{th} moment of a section with respect to its centroidal axis
k	a scalar factor
L	the distance from support to the center of opening
M	bending moment
N	normal force
P	normal force or concentrated load
Q	the first moment of area with respect to the neutral axis
R	reaction force
r	distance from center of curvature to point of interest
r_{max}	maximum value of r
r_{min}	minimum value of r
\bar{r}	distance from center of curvature to the centroid of the section
t	thickness of web, or a time variable
U	strain energy density function
V	shearing force
x,y, θ	subscripts refer to x, y or θ direction (or section)

n, m, v	subscripts refer to the related forces N, M or V respectively
α, β, γ	constants used in the curved beam formula
α	reduction factor used in Bleich's solution
θ	certain angle
Γ	total strain energy of the section due to normal stress
τ	shearing stress
ξ	distance variable used in integration
ϵ	normal strain
ϵ	the calibrated value of the threshold strain
ϵ	the corrected value of the threshold strain
ν	Poisson's ratio
σ	normal stress
κ	a scalar factor
$\mu\epsilon$	strain in micro-inch/inch

I. INTRODUCTION

Beams with web openings are widely used in construction of buildings and the other structures. These openings, providing the passage of utilities, weaken the strength of the beam and reinforcement is required to prevent a stress concentration problem in the corner.

In the past few years, several researchers have studied this problem, using both analytical and experimental methods. Some theoretical solutions have been found to be a good approach to find the stresses in the vicinity of the openings. The purpose of this study was to determine the efficiency of inclined reinforcement and to compare the results obtained by approximate analysis to that by experimental measurements.

For experimental purposes, a simply supported I-beam (16 WF 50) with two rectangular openings, each 6" x 9", was used as shown in Figure 1, 2, 3. This beam was loaded at midspan with one concentrated load. Strains at points of interest, including the critical points which were determined by brittle coating analysis, were measured by electrical resistance strain gages.

In the analytical solutions, interest is in the application of the practical methods that are frequently used by engineers. Both the well-known "Vierendeel Analysis" and the "Least Work" methods are used to study the stress around the web openings.

The Vierendeel Analysis has been considered a reasonably accurate method to solve the web opening problems. Assumptions made are similar to those made in the Vierendeel Girder Analysis. For the Least Work

method, the vicinity of a web opening is considered as a rectangular ring with curved corner connections. This ring structure was divided into several segments. The center of the opening is selected as the point of application of the redundants. The stresses at each section consist of two parts, the stresses caused by the applied load and the stresses caused by the statically indeterminate forces. The solution is obtained by minimizing the total strain energy.

The primary objectives of this study were:

1. To construct a solution by Least Work method.
2. To compare the experimental results and the calculation based on Vierendeel Analysis and curved beam formula.
3. To study the efficiency of the inclined reinforcement.

This study was limited to a 16WF 50 beam of A36 steel with two 6" x 9" rectangular web openings centered on the neutral axis of the beam. The beam was subjected to combined bending and shear with a fixed value of the moment-shear ratio obtained by placing a given concentrated load at the center of the span. Two loading cases were used during the tests as shown in Fig. 4. One of the openings was reinforced with inclined bars located at the four corners and the other remained unreinforced. The reinforcing bars were welded on one side of the web only.

**THIS BOOK
CONTAINS
NUMEROUS PAGES
WITH DIAGRAMS
THAT ARE CROOKED
COMPARED TO THE
REST OF THE
INFORMATION ON
THE PAGE.**

**THIS IS AS
RECEIVED FROM
CUSTOMER.**

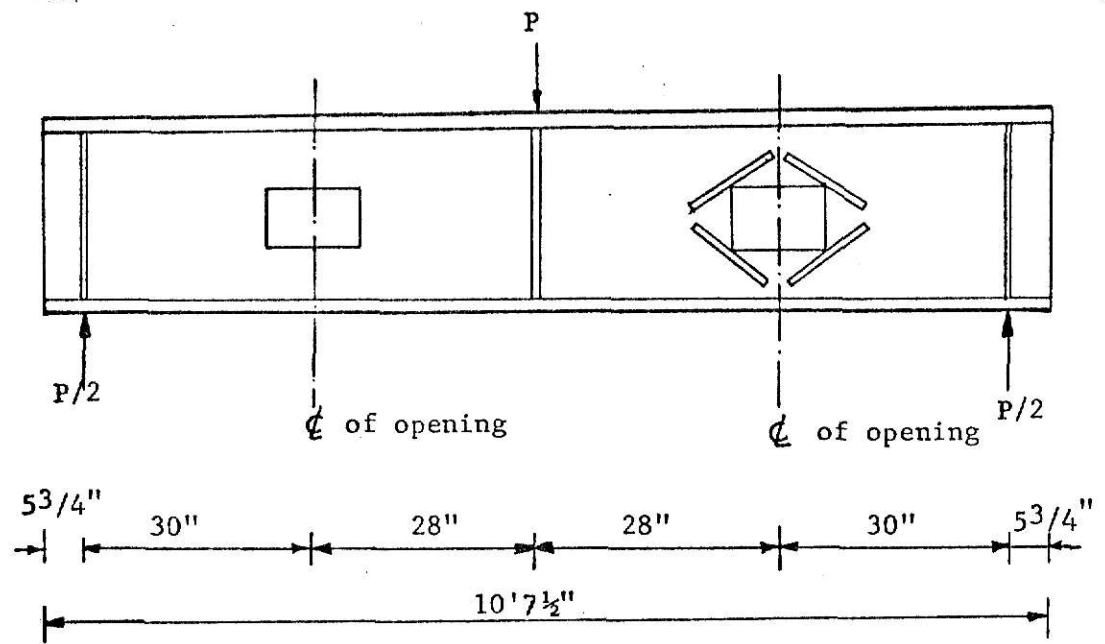


Fig. 1 Simply Supported Beam

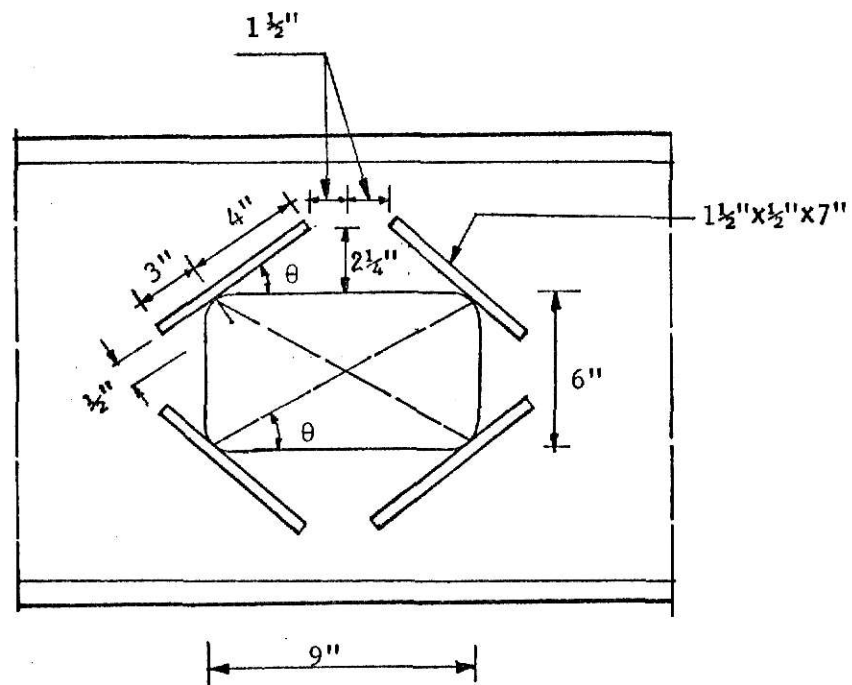
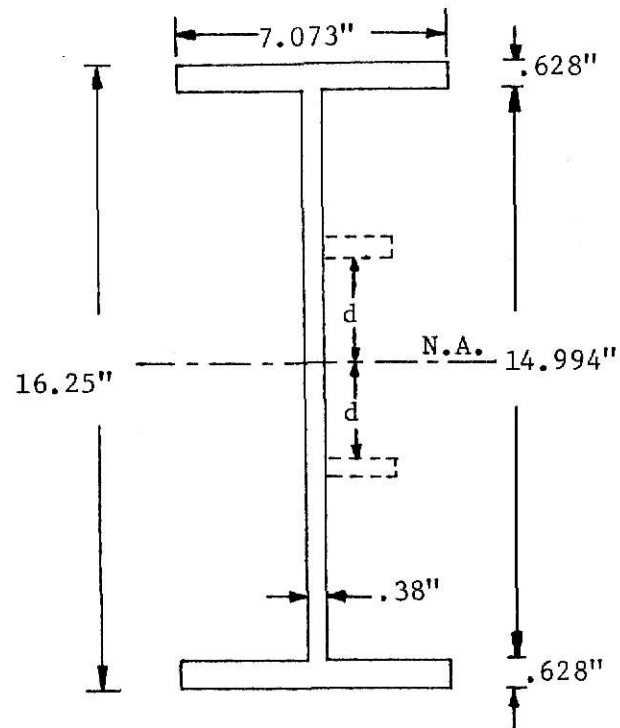


Fig. 2 Web Opening and Reinforcing Details



d: varies as in
different cross
sections

Fig. 3. Beam Cross-Section Details

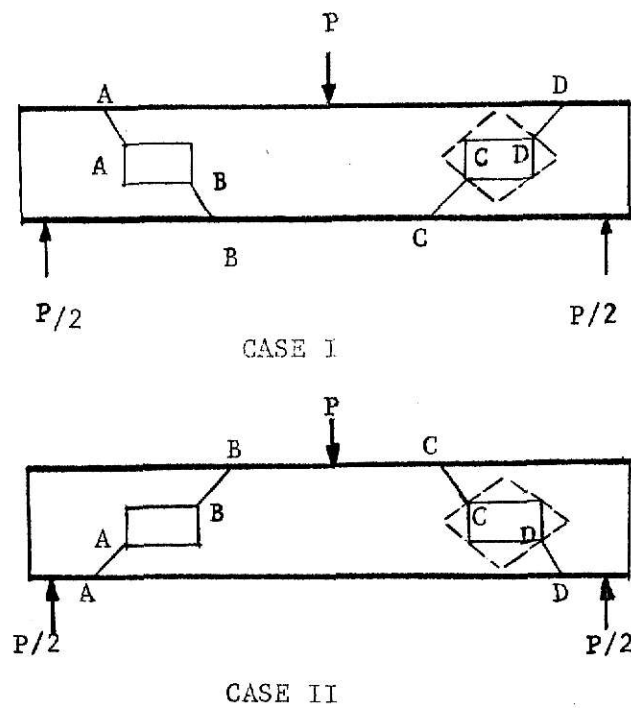


Fig. 4 Two Loading Types

II. LITERATURE SURVEY

In the past few years, many papers concerning the problem of stress concentration due to web opening of a beam have been published. Engineers and researchers made a concentrated effort to develop analytical and experimental information on steel beams with web openings. Some practical methods of solution have been developed.

In the 1920's Muskhelishvili (1) developed a method to solve the stress distribution problem in a plane or thin plate which is weakened by a hole. In 1958, Heller, Brock and Bart (2) presented a solution by using complex variables associated with Muskhelishvili's method for the stress analysis of a uniformly loaded plate with a rectangular opening. Four years later they published a paper using the same technique to investigate the stress around a rectangular opening with rounded corners in a beam subjected to bending and shear (3). They found that the maximum value of the boundary stress is a function of both aspect ratio (height to width) and corner radius.

Bower (4, 5), in 1966, presented two papers using theory of elasticity and complex variable techniques to solve the stress distribution problem of an I-beam with a web opening. He reached the conclusions: that (a) the stress distribution near the hole in uniformly loaded beams is quite different from that in the beam without the hole, (b) both the size of the hole and the moment-shear ratio at the hole have a great influence on the applicability of the analysis, (c) the solution is valid for predicting stress near the opening providing the depth of opening does not exceed half the web depth. He also used the "Vierendeel Analysis" method to calculate the stresses in the vicinity of the hole and

found that this method had good accuracy for predicting the stresses around the hole, except for the stress concentrations near the corners. From his experimental studies it was found also that both the theory of elasticity and the Vierendeel method show reasonable accuracy. The Vierendeel method is simpler, as compared with the theory of elasticity.

Recently, a finite element method has been used to solve this problem. It is an accurate but more expensive method compared to other more time consuming methods.

Researchers at McGill University, Redwood and McCutcheon (11), have completed a series of theoretical and experimental studies of web openings in beams. They concluded that (a) stress concentrations always occur at the corners under all loading conditions, (b) experimental studies verify that the Vierendeel Method is satisfactory and can be used to predict the stress around the rectangular opening at ultimate load, (c) deflections for one or two circular openings are 10 percent greater than that estimated by ignoring the presence of the opening.

At Kansas State University, Arora (6) and Chen (7) completed the experimental stress analysis of an I-beam with a web cutout. Both electrical resistance strain gages and photoelastic techniques were used to determine the stress around the opening. They found that (a) both methods are effective, (b) experimental studies agree with the Vierendeel Method, (c) the normal bending stress distribution is non-linear in a region extending from the edge of the opening about equal to the depth of the beam from the opening, and straight beam theory can not be used to predict normal stresses in this region, (d) greater shearing stresses occur than are predicted by straight beam theory, (e)

"Shear-Difference" method is considered an excellent method for computing the stresses at the interior points of a structure in photo-elastic analysis.

In recent years, there were several researchers at Kansas State University who completed a series of theoretical and experimental analyses. Some reports and theses were completed and papers published (8, 9, 10). Among these studies, Vierendeel Analysis, elastic analysis and ultimate strength analysis were used to analyze the stresses around web openings with and without reinforcement. Valuable results were obtained and directions for further studies were indicated.

III. METHODS OF ANALYSIS

It is assumed that the material is homogeneous, isotropic and elastic. Based on this the following methods were developed.

A. Least Work Method

(a) Ring Structure

From the results of experimental and theoretical analysis, it is known that the stress distribution curve does not lie close to that given by straight beam theory (16,17). For a better assumption, the vicinity of the opening is considered as a rectangular ring with the four corner connecting blocks taken to be curved beams (14,9), as explained in Fig. 5.

B	A	H
C		G
D	E	F

curved beam: B,D,F,H

straight beam: A,C,E,G

Fig. 5 A Partition of Ring Structure

This ring structure is divided into 56 sections, as shown in Fig. 6, for convenience in numerical calculation. The center of the opening is selected as the point of application of the redundants that can be found by minimizing the strain energy of the ring structure.

(b) Corner Connecting Blocks

(1) Effective Width

Typical cross section around the corner of the web opening is shown in Fig. 7.



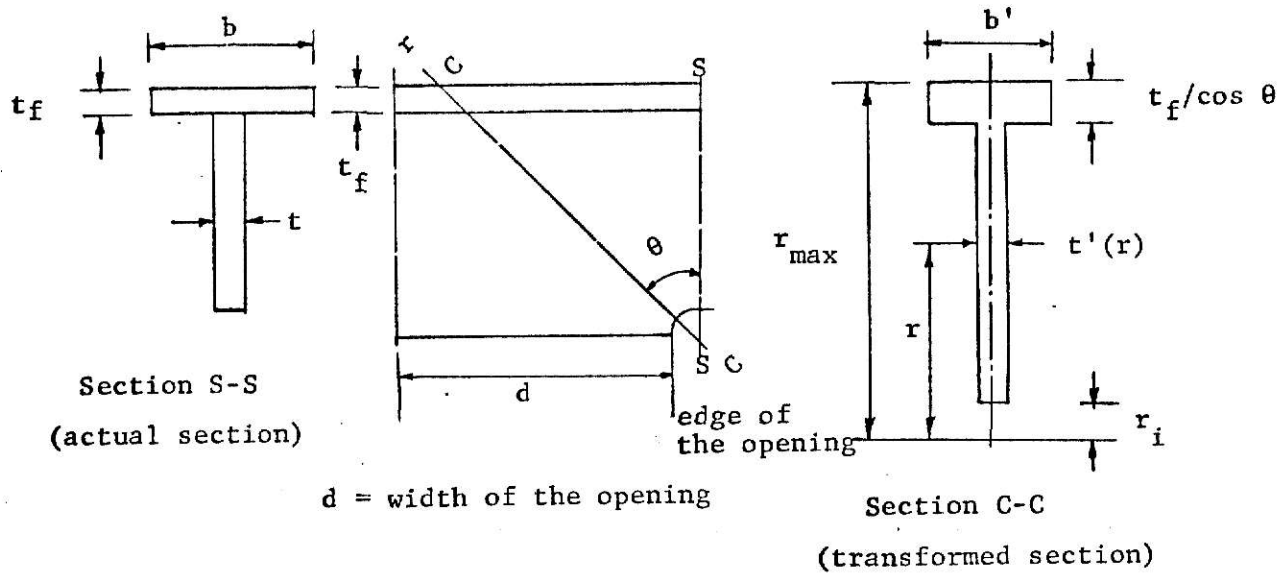


Fig. 7 Cross Section of Curved Beam

If the points of interests are close to the edge of the circular fillet, the principal stress is almost perpendicular to the radius. For those points close to the flange and inside the flange the actual principal stress is in the horizontal direction, which is not in the normal direction of the plane of interest, thus the thickness of the web and the width of the flange should be reduced. From the stresses transformation formula,

$$\sigma_{\theta} = \sigma_x \cos^2 \theta . \quad (1)$$

This leads to an effective width b' as shown in Fig. 7 is given by

$$b' = b \cos^2 \theta . \quad (2)$$

The effective thickness of the web $t'(r)$ at distance r as shown in Fig. 7 is also given by

$$t'(r) = t \cos^2 \theta ; \quad (3)$$

where $\theta(r)$ is assumed to be

$$\theta(r) = \left[\frac{r - r_i}{r_{\max} - r_i} \right]^2 \theta, \quad (4)$$

empirically (see the crack patterns shown in Fig. 12).

(2) Normal Stress

Using Curved Beam Theory (15) to get an approximate formula, let the normal stress at y , the distance from the centroid of the section to the point of consideration, be expressed by

$$\sigma(y) = \frac{P}{A} + \frac{My}{I} + \alpha(1 + \beta y + \gamma y^2), \quad (5)$$

where constants α , β and γ , which satisfy the following eqns. (6), (7) and (16) give the best normal stress distribution of the assumed form. Statical equilibrium condition yields

$$\int_A (1 + \beta y + \gamma y^2) dA = 0, \quad (6)$$

and

$$\int_A (1 + \beta y + \gamma y^2) y dA = 0. \quad (7)$$

Note that $\int y dA = 0$, since the origin is the centroid of the cross section.

Eqns. (6) and (7) are reduced to

$$\int dA + \int y^2 dA = 0, \quad (8)$$

and

$$\beta \int y^2 dA + \gamma \int y^3 dA = 0. \quad (9)$$

Solving eqns. (8) and (9) simultaneously, leads to

$$\beta = \frac{AI_3}{(I_2)^2}. \quad (10)$$

and

$$\beta = \frac{-A}{I_2} . \quad (11)$$

In which

$$A = \int_A dA, \quad (12)$$

$$I_n = \int_A y^n dA, \quad (13)$$

and n is an integer.

The total strain energy of the section due to normal stress is found to be

$$\Gamma = \frac{1}{2E} \int_A \sigma^2(y) r(y) dA. \quad (14)$$

Substituting eqn. (5) into eqn. (14), yields

$$\Gamma = \frac{1}{2E} \int_A \left\{ \frac{P}{A} + \frac{My}{I} + \alpha(1+\beta y+\gamma y^2) \right\}^2 r(y) dA \quad (15)$$

The minimum value of Γ requires

$$\frac{\partial \Gamma}{\partial \alpha} = 0. \quad (16)$$

From eqn. (15), the above equation becomes

$$\frac{1}{E} \int \left\{ \frac{P}{A} + \frac{My}{I} + \alpha(1+\beta y+\gamma y^2) \right\} (1+\beta y+\gamma y^2) r(y) dA = 0. \quad (17)$$

For convenience, let

$$\alpha = M\alpha_m + P\alpha_p. \quad (18)$$

Considering the case of pure bending, i.e., $P=0$ and $\alpha = M_m$, eqn. (17)

is reduced to

$$\frac{1}{E} \int \frac{My}{I} (1+\beta y+\gamma y^2) r(y) dA + \frac{M_m}{E} \int (1+\beta y+\gamma y^2)^2 r(y) dA = 0. \quad (19)$$

Solving eqn. (19) for α_m , one obtains

$$\alpha = \frac{-\int \frac{\gamma}{I} (1+\beta\gamma+\gamma^2) r(y) dA}{\int (1+\beta\gamma+\gamma^2)^2 r(y) dA} . \quad (20)$$

Similarly, considering $M=0$ and $\alpha = P\alpha_p$, yields

$$\alpha_p = \frac{\frac{1}{A} \int (1+\beta\gamma+\gamma^2) (y) dA}{(1+\beta\gamma+\gamma^2)^2 r(y) dA} . \quad (21)$$

Eqns. (20) and (21) are simplified to the following forms

$$\alpha_m = \frac{-C_m}{DI_2} , \quad (22)$$

and
$$\alpha_p = \frac{-C_p}{DA} , \quad (23)$$

by defining

$$C_m = I_2(1+\bar{\tau}\beta) + I_3(\bar{\tau}\gamma+\beta) + I_4\gamma , \quad (24)$$

$$C_p = I_2(\beta+\bar{\tau}\gamma) + I_3 + \bar{\tau}A \quad (25)$$

and

$$D = I_5\gamma^2 + (2\beta+\bar{\tau}\gamma)\gamma I_4 + \{\beta^2+2\gamma(1+\bar{\tau}\beta)\} I_3 + \{\bar{\tau}(\beta^2+2\gamma) + 2\beta\} I_2 + \bar{\tau}A. \quad (26)$$

(3) Shearing Stress

The approximate shearing stress can be obtained by requiring equilibrium of the freebody above section A-A shown in Fig. 8a.

By considering Fig. 8b, it can be seen that

$$\tau(r) = \frac{1}{rb(r)d\theta} \left[\int_r^R (V\bar{\tau}d\theta) \left\{ \frac{\xi-\bar{\tau}}{I} + \alpha_m(1+\beta(\xi-\bar{\tau})^2 + \gamma(\xi-\bar{\tau})^2) \right\} b(\xi)d\xi - \int_r^R \tau(\xi)b(\xi)d\theta d\xi \right] . \quad (27)$$

For an approximate solution, ignore the term $\int_r^R \tau(\xi)b(\xi)d\theta d\xi$,

assume (see reference 19)

$$\tau(r) = \frac{kVF}{rb(r)} \int_r^{r_0} \left\{ \frac{\xi - \bar{r}}{I} + \alpha_m (1 + \beta(\xi - \bar{r}) + r(\xi - \bar{r})^2) \right\} b(\xi) d\xi. \quad (28)$$

The coefficient k in eqn. (28) can be calculated by using the condition

$$\int_r^{r_0} \tau(r) b(r) dr = V. \quad (29)$$

The function of strain energy density per unit length along the arc of the axis of the structure due to shearing stress (see Fig. 6) for a section at θ is given by

$$U = \frac{1}{2G} \int \tau^2(r) rb(r) dr. \quad (30)$$

Note that in eqns. (28) to (30), $b(r)$, α_m , β and γ are functions of θ .

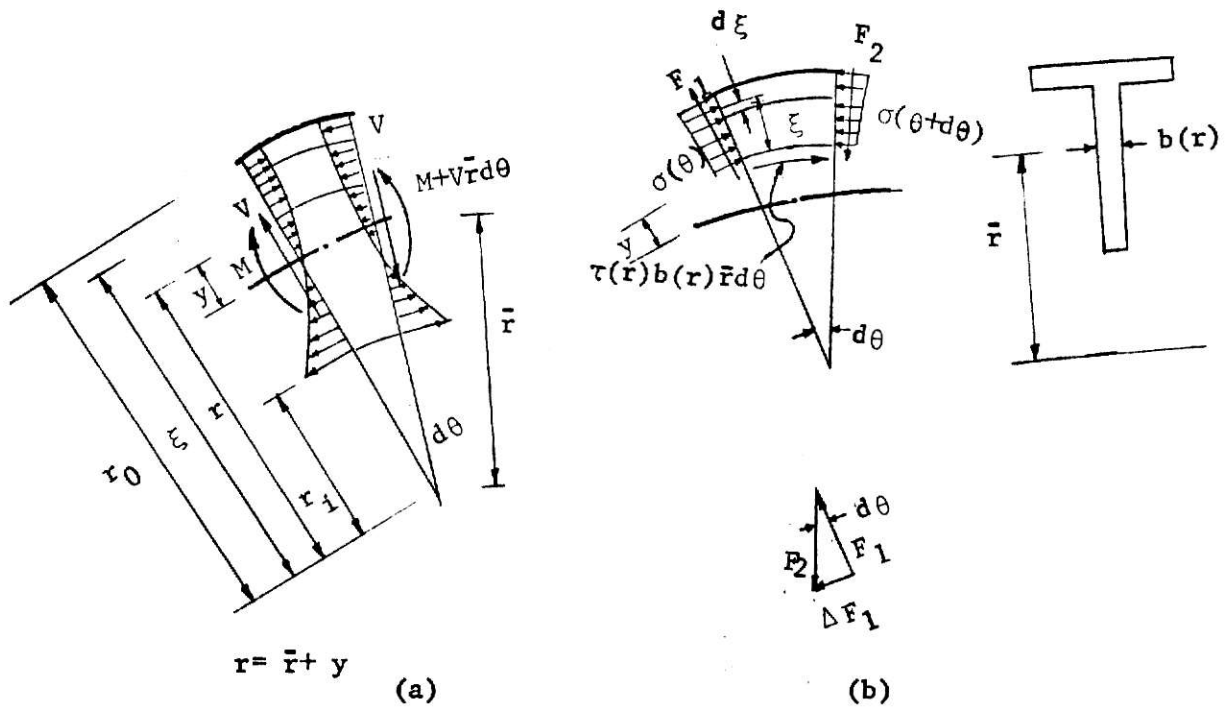


Fig. 8 Freebody Diagram of a Curved Beam

(c) Strain Energy

(1) Corner Connecting Blocks

The strain energy of each section in the corner connecting blocks can be computed by

$$\frac{dU}{d\theta} = \int \frac{1}{2E} \sigma^2(y) r(y) dA + \int \frac{1}{2G} \tau_{\theta}^2(y) r(y) dA \quad (31)$$

By using eqns. (5) and (28), eqn. (31) can be written in the form

$$\frac{dU}{d\theta} = \frac{M^2}{2E} U_m + \frac{N^2}{2E} U_n + \frac{MN}{E} U_{mn} + \frac{V^2}{2G} U_v \quad (32)$$

The computation of U_m , U_n , U_{mn} , and U_v can be calculated using a numerical method and the electronic computing machine.

(2) Straight Beam Part

The strain energy for straight beam part was calculated by the well-known formula

$$U = \int \left(\frac{M^2}{2EI} + \frac{N^2}{2AE} + \frac{\kappa V^2}{2GA} \right) ds, \quad (33)$$

where κ is a shape factor given by

$$\kappa = \frac{A}{I^2} \int A \frac{Q^2(y)}{t} dy, \quad (34)$$

and

$$Q(y) = \int_y^{y_{\max}} b(\xi) \xi d\xi. \quad (35)$$

B. Vierendeel Method

This method provided a simple way to solve the web opening problem and to give a reasonable result. It assumes that the upper and lower T-beams of the opening have their points of inflection at the center line of the opening. This leads to the results as shown in Fig. 9a.

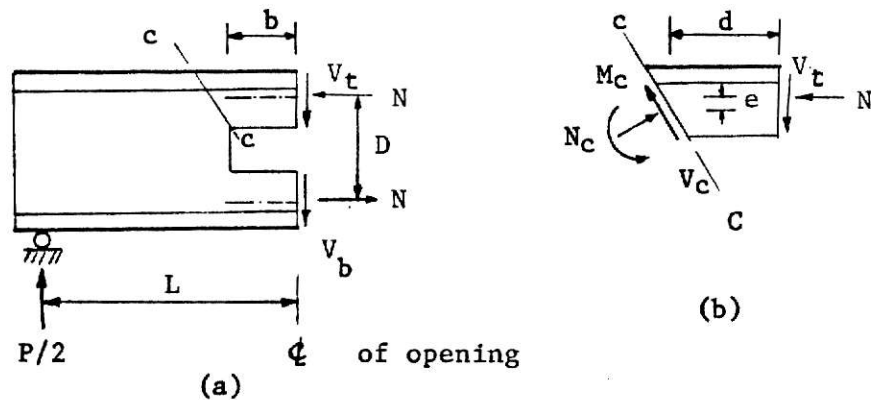


Fig. 9 Freebody Diagram for Vierendeel Analysis

The thrust force N reads

$$N = \frac{PL}{2D} \quad (36)$$

with D the distance between the centroid of the upper and lower T-sections.

If the opening is symmetric,

$$V_t = V_b = P/4. \quad (37)$$

Otherwise, it should be calculated according to the stiffness of the T-beams. From Fig. 9b, the reaction forces N_c , V_c and M_c can be obtained by using statical equilibrium conditions. For those sections which lie in the straight beam portions of the opening, the stress at any points y can be calculated by the conventional method

$$\sigma(y) = \frac{N_c}{A} \pm \frac{M_c y}{I} \quad (38)$$

and

$$\tau(y) = \frac{V_c Q(y)}{t(y) I} \quad (39)$$

The stress distribution of the sections at the corners could be calculated by using eqns. (5) or Winkler's Curved Beam Theory (18) for a better approximation. The calculation of the normal stress at the critical sections of the tested beam is given in Appendix I. The results were used to compare with the experimental measurements as shown in Table 6.

IV. EXPERIMENTAL STUDIES

A. Brittle-Coating Method

a. Introduction

The Brittle-Coating Method is based on the perfect adhesion of a coating with brittle characteristics and predictable threshold strain. It gives whole field data for determining the directions and approximate magnitudes of the principal stresses. It is also very useful in finding the locations of the maximum stresses. Since it can be applied to the actual component, it is a direct and simple method for experimental stress analysis.

b. Procedures for Stress-Coating Method (12, 13)

(1) Surface Preparation

Grinders, sand paper and steel wool were used to make the surface smooth and flat. Dirt and grease were removed from the surface by using solvents which leave no residue.

(2) Spraying the undercoating

Aluminum reflecting undercoating was used according to manufacture's bulletin. After 10 to 20 minutes for drying, brittle lacquer was sprayed.

(3) Spraying the Coating

Coatings were sprayed on the beam with 3 to 4 passes each time. After each spraying, the technician waited about 5 minutes and then sprayed again until the color matches the desired thickness. Table 1 and Fig.10 show the relationship between threshold strain, coating thickness and number of spraying passes. It was found that the threshold strain is not sensitive to coating thick-

Table 1 Brittle-Coating Calibration Bar Test Records

No. of Passes	Test No. 1		Test No. 2	
	Thickness (in.)	Threshold Strain($\mu\epsilon$)	Thickness (in.)	Threshold Strain($\mu\epsilon$)
12	.007	930	.010	670
14	.010	1100	.009	880
16	.012	840	.011	590
18	.013	540	.016	670
20	.015	670	.015	670
22	.016	760	.013	840
Average	.012	780	.012	720
Remarks	Items	Spray	Test	
	Date	7/3/75	7/4/75	
	Time	9:30PM	9:30PM	
	Temp.	79 F	79 F	
	R.H.	69%	68%	

ness during these tests.

(4) Testing

The dust was removed just before testing by gently and lightly dusting off the surface with a soft hair brush. The calibration bar was kept close to the test part during drying and testing. It experienced the identical time, temperature and relative humidity history that the test part experienced.

(5) Crack Detection

The crack can be better observed by using a direct light source at oblique incidence to the surface and normal to the crack line. Some other methods were also used to help in detecting the crack pattern: i) using electrified particle inspection, ii) using the red dye etchant, iii) using the protective cream associated with the red dye etchant and electrified particle. The first two methods were developed by Magnaflux Corporation and widely used by engineers and the third method was tried by the author and it was found to be helpful for detecting the crack.

Procedure used by the protective cream associated with the red dye etchant and the electrified particle: i) After the cracks developed, protective cream was slightly filled into the cracks and then a tissue was used to erase the extra cream. ii) The red dye etchant was brushed uniformly on the whole surface of the coating and then a tissue was used to erase the surface. iii) The loads were released to make the crack smaller and then the electrified particles were sprayed (by air pressure up to 15 Psi) as soon as possible. Picture of this white crack pattern with red background

were taken using KODAK Panatomic - X (Fx 135-20) black and white film.

For each loading level, the crack line tips were found using a flash light and a countour line was drawn by a steel scribe.

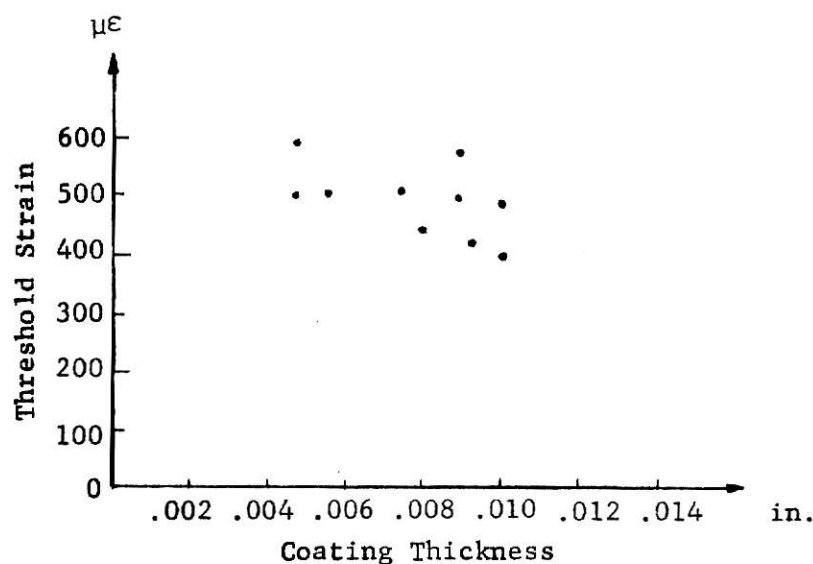


Fig. 10 Threshold Strain Verses Coating Thickness

c. Beam Testing

TENS-LAC BRITTLE LACQUER TL-500-80 was chosen according to the estimated laboratory condition and selection chart shown in Bulletin TL-201 of Photolastic Inc.

For loading cases, only case I* was used during the test. Fig. 11 shows the load-time history of the tests. At each loading level, the coating threshold strain was calibrated by a calibration bar test. The threshold strain was found by averaging the adjusted values, according to reference temperature and humidity, of each calculation bar threshold strain. Table B shows the calibrated threshold strain and the corresponding relative humidities at each loading level.

* see Fig. 4

The threshold strain due to the difference of loading time of the calibration bar tests and the beam tests was corrected by using an approximate empirical equation (12).

$$\epsilon_t^{**} = [1 + .05 (\log_{10} t)^2] \epsilon_t^*, \text{ for 1 to 1,000 Sec.} \quad (40)$$

In which

ϵ_t^{**} is the corrected value of the threshold strain

ϵ_t^* is the calibrated value of the threshold strain

t is the time necessary to apply the load to the specimen

It was found that this correction is relatively small compared to that due to temperature and relative humidity.

Countour lines of the tips of the cracks at each loading level were drawn and their locations in the critical radial section were also measured.

The photographs of crack patterns of two corners are shown in Fig. 12 and the traced countour lines are shown in Figs. 13 and 14. The measured data were used in the computation of stress distributions in the critical sections, at a loading level of 25 Kips, as shown in Appendix II. The results were used to compare with those obtained from theory and the electrical resistance strain gage method.

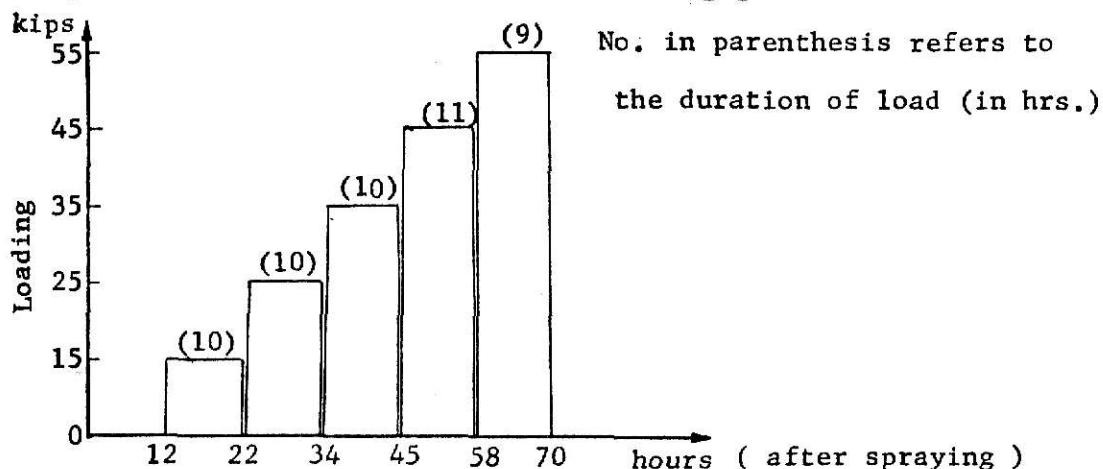
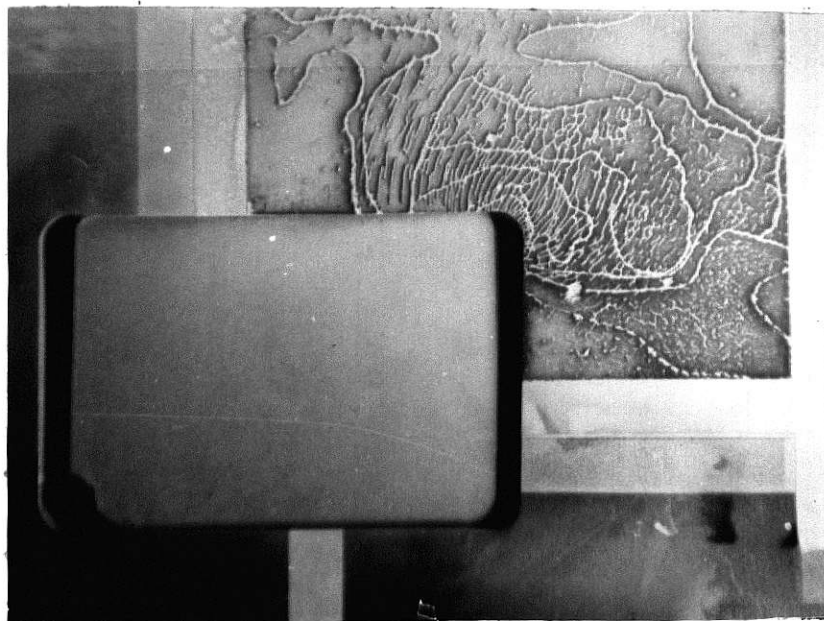


Fig. 11 Loading Vs. Time in Brittle-Coating Beam Test



a. Unreinforced Opening



b. Reinforced Opening

Fig. 12 Photographs of Stress-Coating Crack Pattern
and Contour Lines

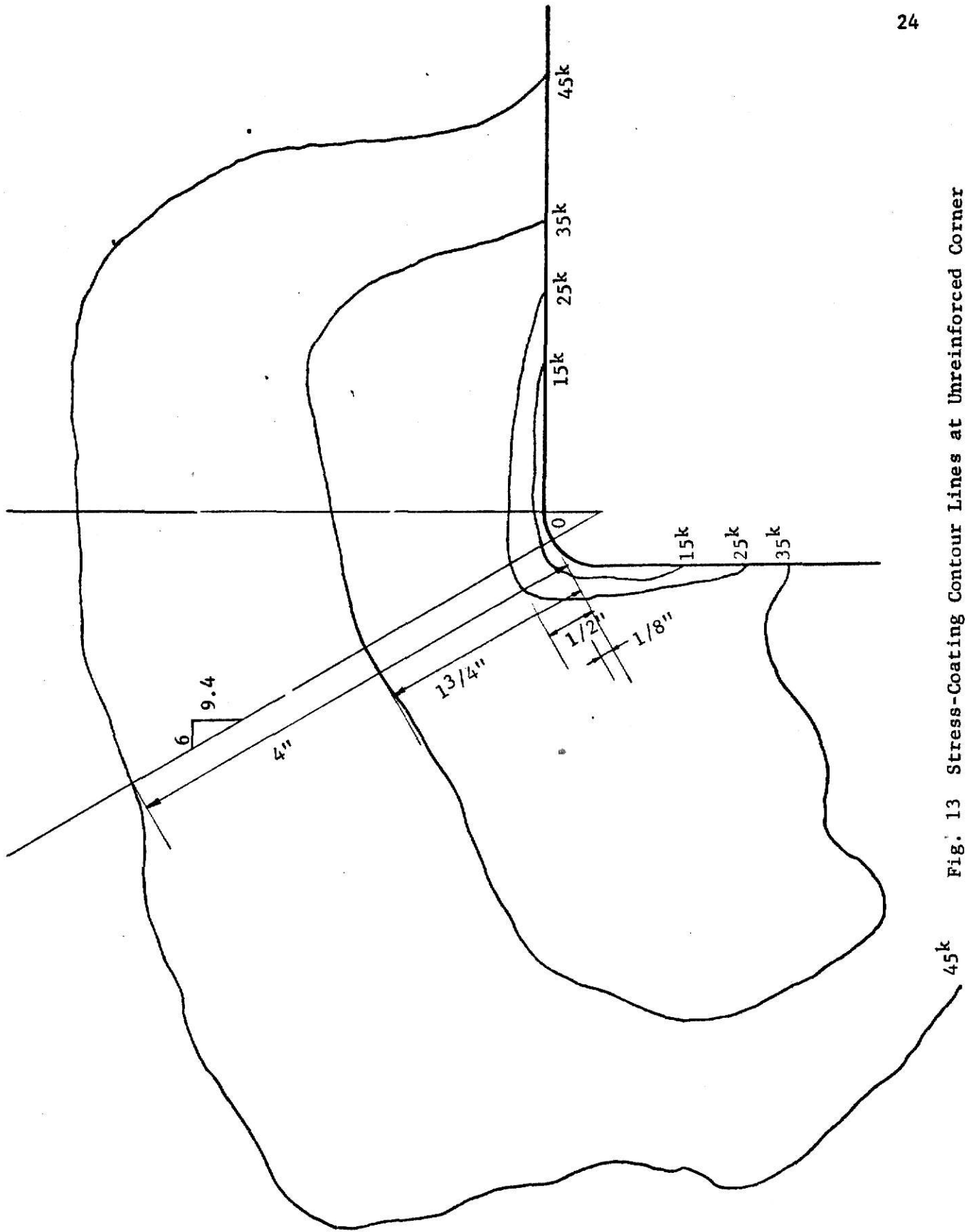


Fig. 13 Stress-Coating Contour Lines at Unreinforced Corner

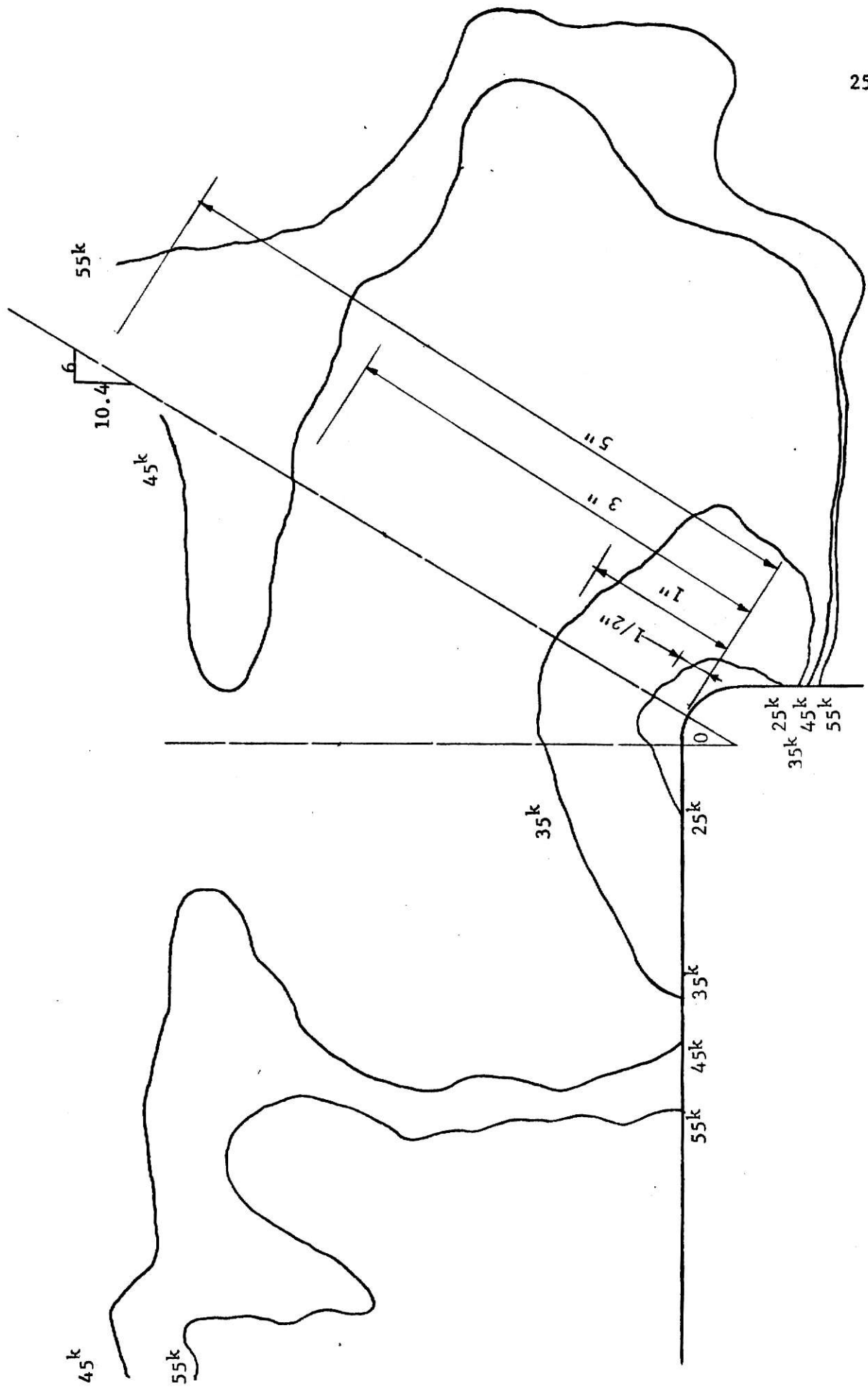


Fig. 14 Stress-Coating Contour Lines at Reinforced Corner

B. Electrical Resistance Strain Gage Method

This method is based on the linear relationship between change in electrical resistance of the gage and the strain in the direction of the gage when the strain is small. The brittle-coating tests, as described in the previous section, show that the most critical points around the opening lie near the corners and were located about 33° from vertical for unreinforced corner A and 30° for reinforced corner D as shown in Figs. 13 and 14.

Twenty Budd C12-1x1-M75C (active gage length of 1/8 in.) one dimensional strain gages, two Budd C6-124D-R3Y delta rosettes and two C6-121-R3C delta rosettes (1/4 in. active gage length of each element) were used to investigate the normal stress along sections A, B, C and D as indicated in Fig. 15.

The strain gage readings were recorded for five different loading levels: 5 kips, 10 kips, 15 kips, 20 kips and 25 kips. Each loading level has two values corresponding to applied loads and released loads. The measured data were linearly corrected to avoid the accumulation of temperature strain in each gage and were fitted by the least square method. Typical loading Vs. strain relationships of a number of sample strain gages are shown in Fig. 16. The corrected data are shown in Tables 3 and 4. It can be seen that all the strain gages yield an almost linear relationship between loading and strain.

The stresses at the extreme points of the section are uniaxial and can be expressed by

$$\sigma = E \epsilon \quad (41)$$

where σ = Normal Stress

E = Young's Modulus (29×10^6 psi was used)

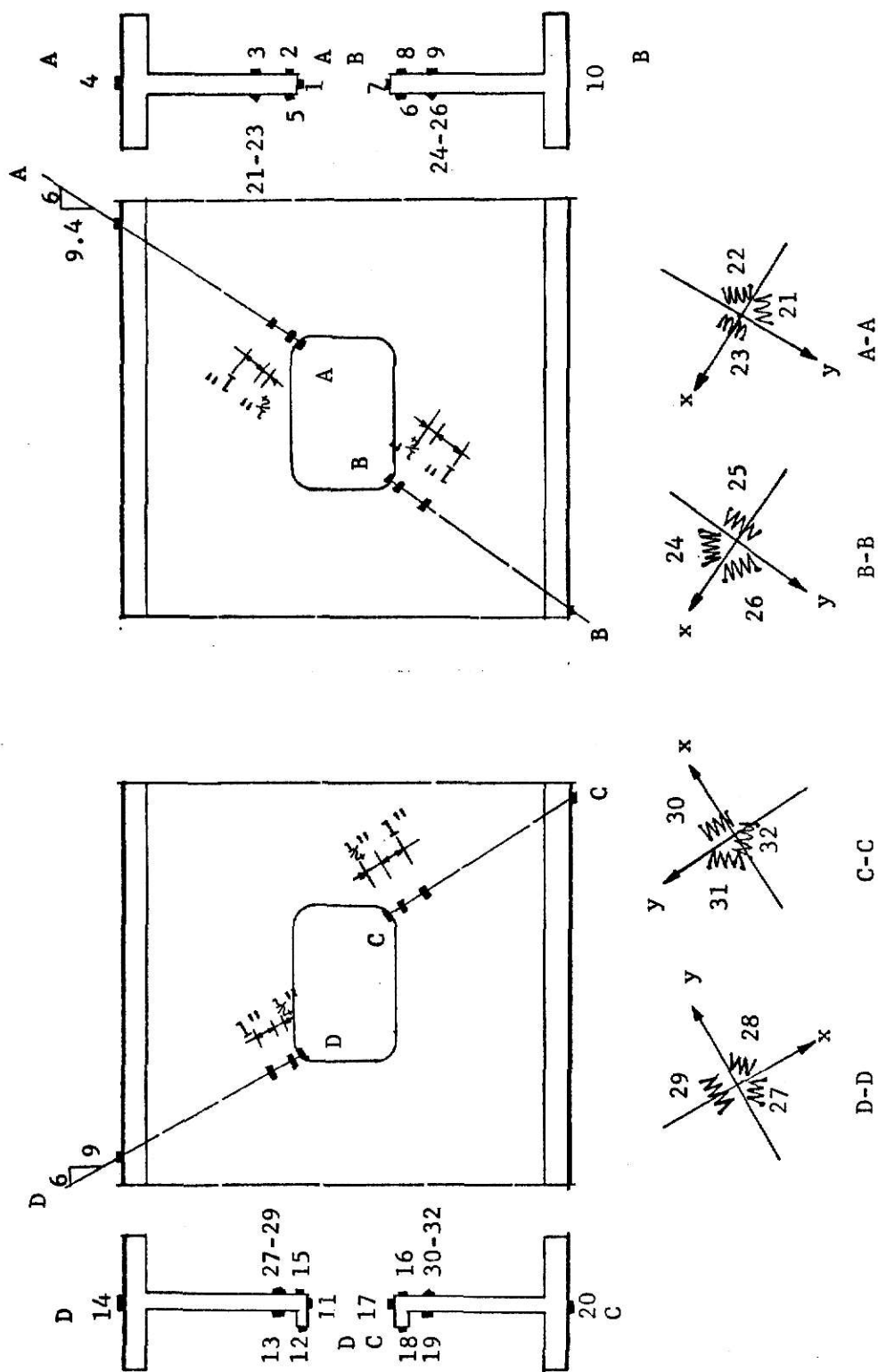


Fig. 15 Strain Gage Locations and Rosette Details

ϵ = Strain Gage Readings

The stresses at the interior points of the section are biaxial and can be expressed by

$$\sigma_x = \frac{E}{1-\nu^2}(\epsilon_x + \nu\epsilon_y), \quad (42)$$

and

$$\sigma_y = \frac{E}{1-\nu^2}(\nu\epsilon_x + \epsilon_y). \quad (43)$$

In the above x, y are the directions of interest, and

$\sigma_{x,y}$ = Stress in x or y direction,

$\epsilon_{x,y}$ = Strain in x or y direction,

E = Young's Modulus,

ν = Poisson's ratio.

In the interior, only the points with a rosette can provide information enough to determine the magnitude and direction of principal strains.

For rosette analysis, the transformation formula of strains is

$$\epsilon_\theta = \frac{\epsilon_x + \epsilon_y}{2} + \frac{\epsilon_x - \epsilon_y}{2} \cos 2\theta - \frac{\gamma_{xy}}{2} \sin 2\theta, \quad (44)$$

In which, x and y are preselected reference axes,

and ϵ_θ = normal strain in θ direction of the gage a, b or c ,

$\epsilon_{x, y}$ = normal strains in x or y direction (tensile strains are positive),

θ = angle between the x axis and the direction of the gage of interest,

γ_{xy} = shearing (It is positive if the 90° angle will be reduced by γ_{xy} strain with respect to xy axis.

Substituting the strains $\epsilon_a, \epsilon_b, \epsilon_c$ and the corresponding angle θ of each strain gage of a rosette into eqn. (44), the values of ϵ_x, ϵ_y and γ_{xy} at each point can be determined. The calculated results were used

for determining the principal stresses and their corresponding directions.

A computer program for this purpose was developed and its results are shown in Table 4.

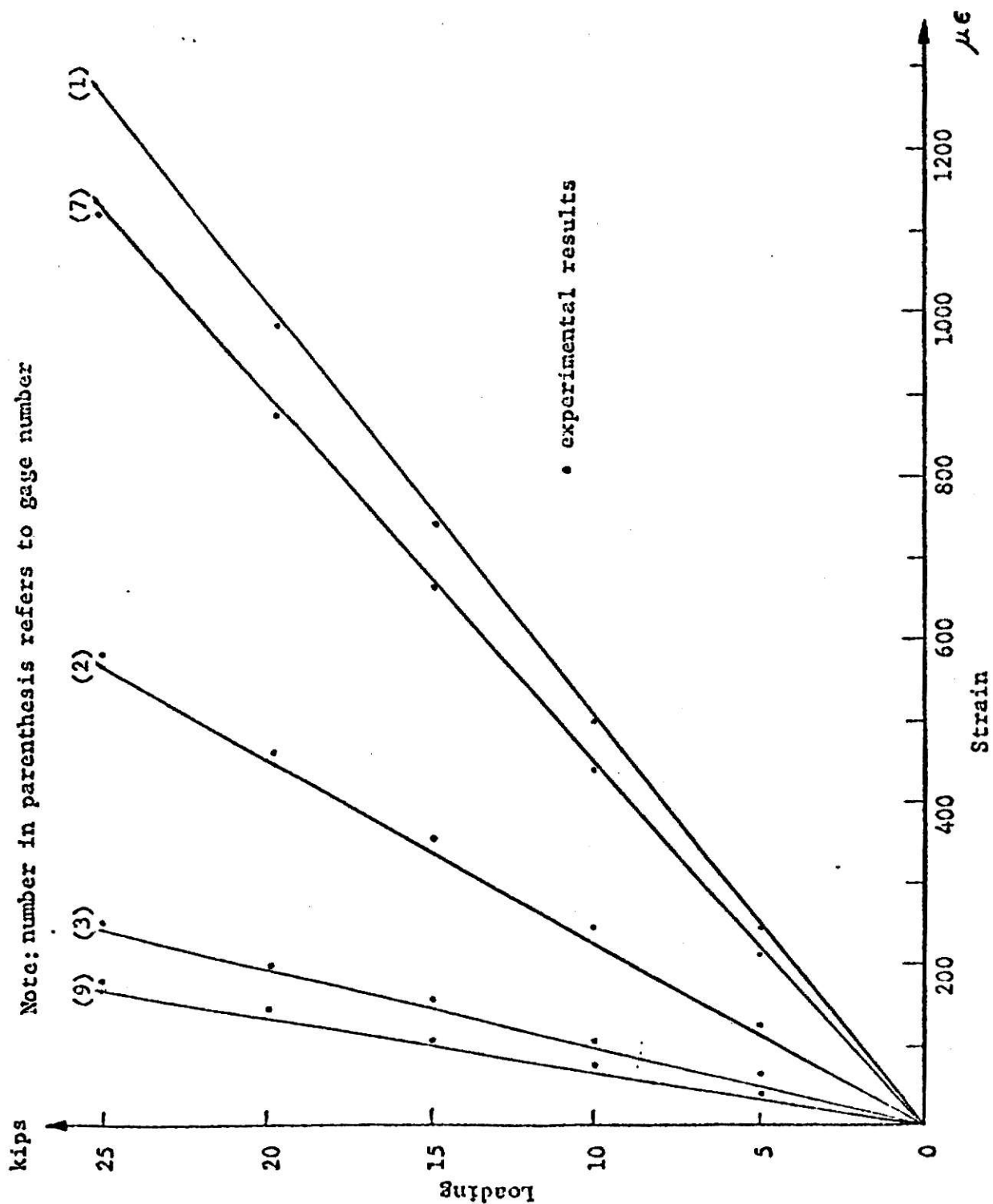


Fig. 16 Typical Strain-Loading Diagram of Strain Gage Measurements

Table 2 Corrected Strain Gage Readings for Loading Case 1

No.	5K	10K	15K	20K	25K	20K	15K	10K	5K	25K*
1	-246	-504	-756	-1018	-1282	-1018	-760	-504	-254	-1281
2	-133	-247	-355	-476	-591	-479	-357	-248	-130	-586
3	-70	-119	-166	-223	-257	-210	-165	-119	-73	-253
4	-30	-53	-71	-101	-113	-102	-72	-53	-28	-115
5	-101	-222	-342	-457	-595	-459	-342	-223	-101	-595
6	-50	-87	-171	-223	-299	-227	-148	-84	-50	-299
7	-214	-442	-662	-885	-1124	-896	-671	-445	-222	-1123
8	-122	-211	-309	-423	-522	-422	-301	-211	-121	-515
9	-51	-81	-107	-149	-180	-152	-109	-82	-53	-175
10	41	95	146	186	243	189	148	103	43	242
11	-205	-413	-651	-817	-1026	-820	-612	-418	-209	-1024
12	24	52	77	87	115	90	81	58	30	112
13	-22	-48	-76	-100	-130	-101	-78	-48	-22	-131
14	-21	-41	-64	-90	-116	-91	-66	-42	-21	-116
15	-84	-192	-288	-383	-498	-384	-291	-193	-85	-498
16	-84	-172	-255	-352	-438	-353	-256	-173	-85	-440
17	-189	-375	-556	-738	-930	-742	-558	-374	-189	-926
18	20	36	55	63	98	62	52	34	16	91
19	-8	-20	-34	-46	-62	-48	-36	-23	-11	-63
20	41	93	141	178	232	179	140	97	40	231
21	-34	-65	-96	-130	-161	-137	-100	-66	-38	-161
22	-15	-31	-57	-64	-89	-76	-60	-38	-23	-89
23	-38	-89	-127	-184	-231	-184	-132	-79	-30	-236
24	-8	-8	-10	-8	-13	-19	-15	-15	-8	-12
25	-12	-35	-73	-102	-128	-91	-61	-41	-14	-131
26	-26	-52	-78	-95	-128	-104	-78	-56	-40	-123
27	-45	-97	-138	-186	-235	-189	-141	-96	-46	-235
28	-38	-66	-95	-138	-171	-143	-95	-65	-37	-170
29	4	-20	-40	-57	-71	-61	-44	-18	-4	-79
30	-29	-56	-79	-99	-127	-107	-71	-53	-33	-124
31	-27	-56	-78	-102	-127	-105	-78	-53	-29	-127
32	0	-7	-11	-15	-22	-14	-14	-10	-4	-22

Note:(1) Values in the last column show the experimental results.

(2) Units are in micro-inch/inch.

Table 3 Corrected Strain Gage Readings for Loading Case 2

No.	5K	10K	15K	20K	25K	20K	15K	10K	5K	25K*
1	243	506	754	1018	1260	1019	768	515	259	1264
2	111	222	330	446	557	451	331	222	113	558
3	48	96	144	195	225	197	144	95	50	231
4	3	46	62	85	101	87	63	44	20	107
5	115	237	355	464	587	469	361	240	123	585
6	77	146	202	270	330	263	196	135	76	325
7	204	428	644	873	1092	872	657	434	209	1096
8	93	194	289	411	499	407	294	186	90	507
9	26	52	78	110	138	111	77	51	21	139
10	-44	-98	-144	-199	-249	-200	-144	-96	-41	-251
11	179	386	587	778	986	794	597	395	190	990
12	-9	-34	-57	-74	-97	-78	-58	-33	-12	-101
13	19	44	74	92	120	93	74	46	19	121
14	22	43	59	78	101	79	62	43	22	99
15	78	176	271	359	455	365	279	182	83	459
16	70	155	240	316	397	318	247	160	79	400
17	164	337	515	688	865	711	525	342	169	872
18	-2	-21	-38	-52	-71	-54	-40	-22	-7	-74
19	14	19	32	38	50	38	33	18	13	48
20	-40	-95	-145	-196	-240	-196	-147	-98	-43	-245
21	25	60	86	120	141	118	92	60	31	144
22	19	23	43	68	85	71	55	21	18	87
23	60	99	150	197	247	200	151	100	60	243
24	-1	-1	-1	-4	-4	-3	-1	-2	-2	-3
25	44	53	80	108	138	110	89	55	37	132
26	24	51	76	104	132	109	75	59	18	134
27	50	96	140	193	228	189	134	101	44	230
28	28	61	100	133	166	136	94	65	36	167
29	29	44	63	79	91	81	46	43	34	88
30	19	47	71	98	110	93	64	45	15	116
31	25	55	79	107	141	103	81	50	22	139
32	6	19	24	22	25	21	21	17	4	26

Note: (1) Values in the last column show the experimental results.

(2) Units are in micro-inch/inch.

Table 4 Results of Rosette Analysis

L O A D		ϵ_x	ϵ_y	γ_{xy}	$\frac{\epsilon_x + \epsilon_y}{2}$	$\frac{\sqrt{\epsilon_x^2 + \epsilon_y^2}}{2}$	ϵ_{\max}	ϵ_{\min}	$\theta(\epsilon_x, \epsilon_{\min})$ (degree)
					$+\frac{\gamma_{xy}}{2}$				
C A S E I	A-A	-235.57	-88.33	83.80	-161.95	84.71	-77.25	-246.66	-14.82
	B-B	-131.36	-46.17	-129.08	-88.76	77.33	-11.43	-166.09	28.29
	C-C	-124.50	-57.45	121.41	-90.98	69.35	-21.63	-160.32	-30.55
	D-D	-79.29	-243.67	74.07	-161.48	90.15	-71.33	-251.62	12.12*
C A S E II	A-A	242.64	72.88	-65.90	157.76	91.05	248.81	66.71	-10.61*
	B-B	132.29	42.86	158.52	87.57	91.00	178.58	-3.43	30.28*
	C-C	115.64	71.31	-131.22	93.48	69.26	162.73	24.22	-35.67*
	D-D	87.71	235.95	-72.22	161.83	82.58	244.41	79.25	13.08

Note: 1. Sign of angle is positive if clockwise.

2. Values of θ with a "*" refer to $(\epsilon_x, \epsilon_{\max})$.

3. Unit of strain in micro-in/in.

Table 5 A Comparison List of Critical Normal Stresses

Method of Analysis	LOADING CASE I				LOADING CASE II			
	A-A	B-B	C-C	D-D	A-A	B-B	C-C	D-D
Theoretical	-41.00	---	---	-16.52	---	40.73	31.97	---
Strain Gage	-37.20	-32.57	-26.52	-29.70	36.70	31.78	25.29	28.71
Stress Coating	-31.00	---	---	-24.00	---	---	---	---

(unit in ksi)

V. COMPARISON AND DISCUSSION OF RESULTS

The interest of this study is in the most critical sections and the most critical points near the corners. Fig. 17 shows the normal stress distribution along section D-D and A-A obtained by brittle-coating method.

Figs. 18 and 19 show the results obtained by electrical strain gage measurements. From these data, the principal stress distributions calculated are quite similiar to those obtained from the brittle-coating method only with a slightly higher value.

Results from the strain gage method are more reliable than those obtained from the brittle-coating method. The small errors produced by temperature can be eliminated by using a temperature compensating strain gage, while the coatings exhibit high sensitivity to temperature. For better accuracy with the brittle-coating method, it is recommended that the tests be performed in a well-controlled laboratory in order to get a constant temperature and humidity. In addition, more calibration bars should be used.

Theoretical results and experimental results are compared as shown in Table 5. It can be seen that the stresses at unreinforced corners are about 20% greater than those at reinforced corners.

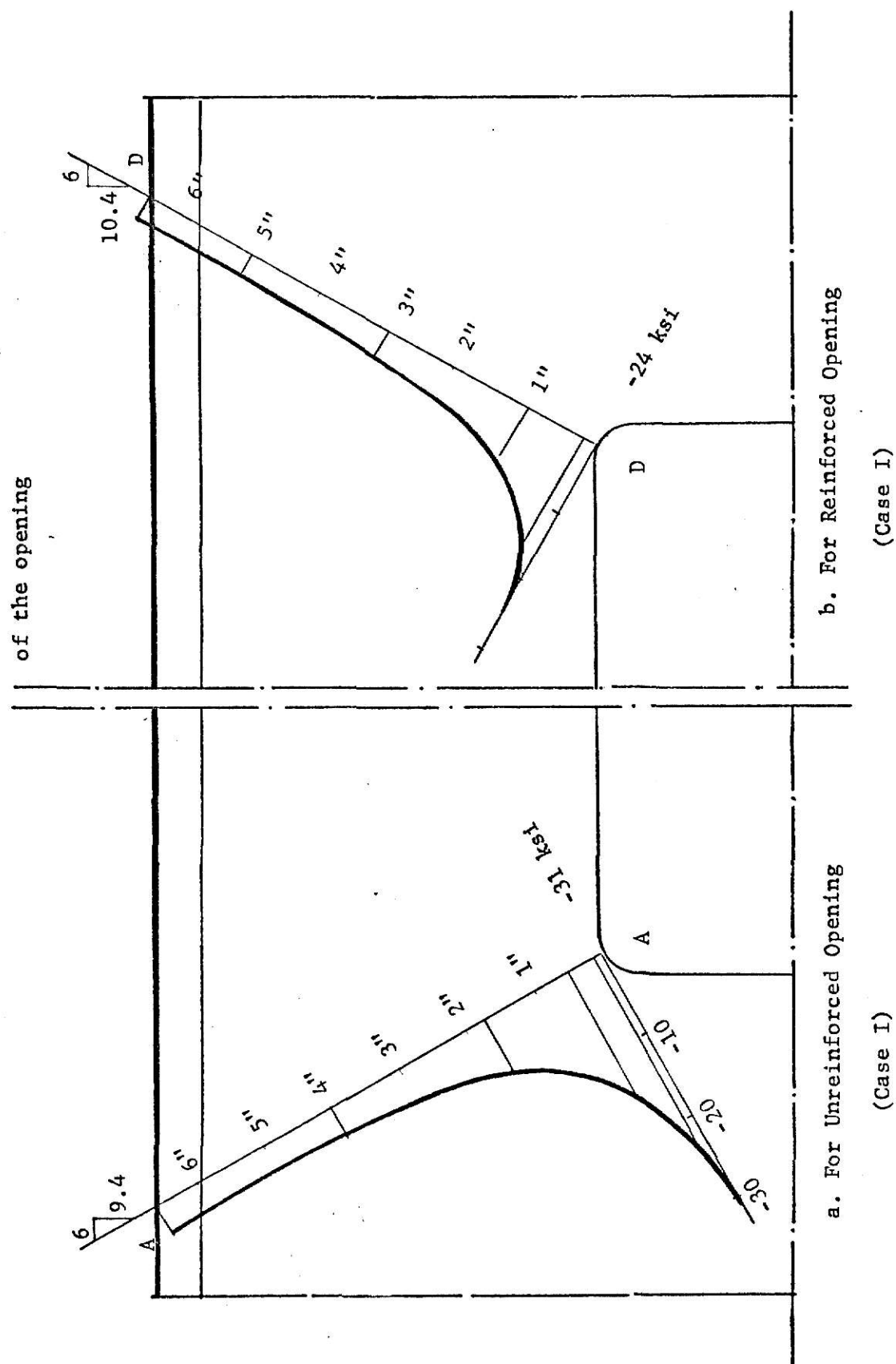


Fig. 17 Normal Stress Distribution Curves by Brittle-Coating Method

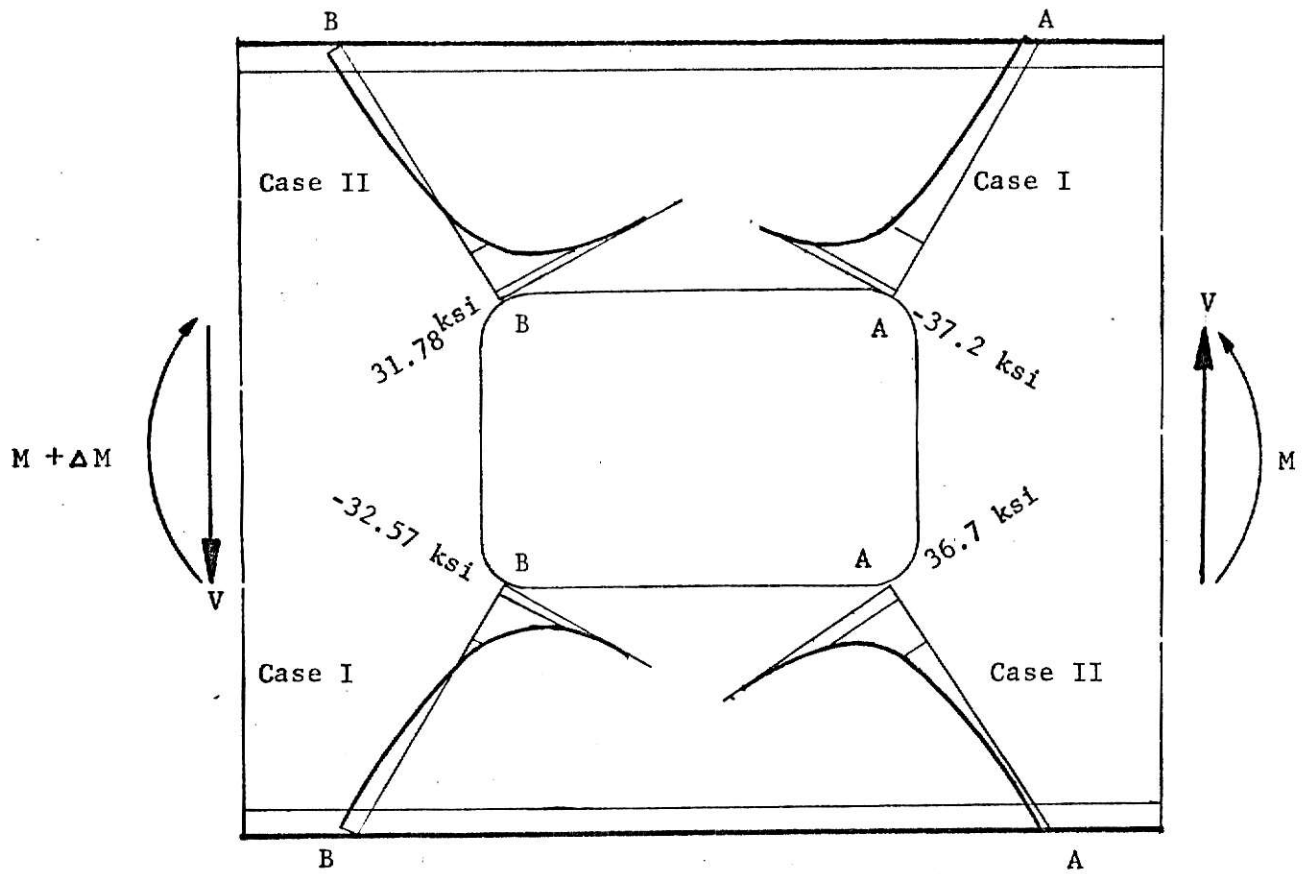


Fig. 18 Normal Stress Curves for Unreinforced Opening by Electrical Strain Gage Method

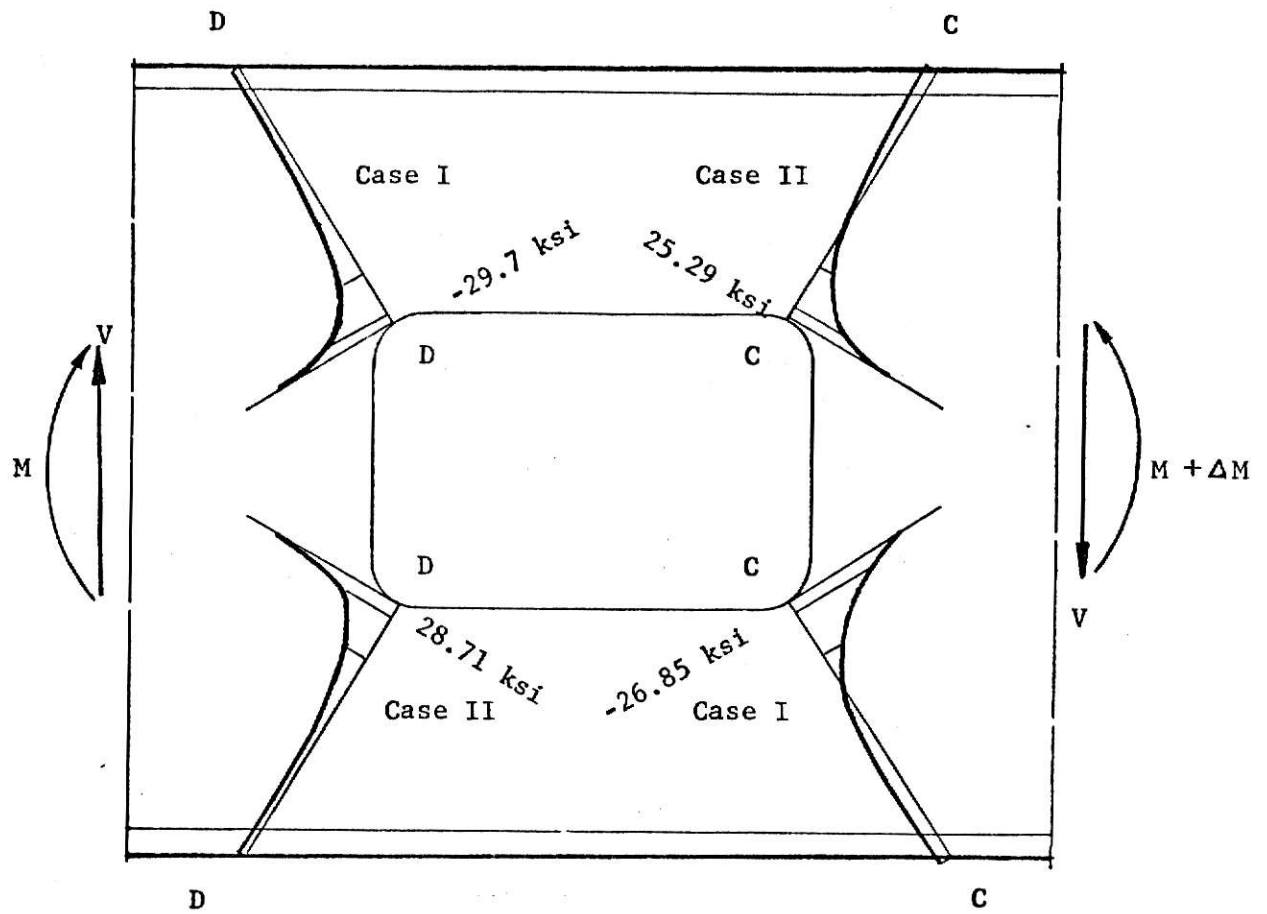


Fig. 19 Normal Stress Curves for Reinforced Opening
by Electrical Resistance Strain Gage Method

VI. CONCLUSIONS

From these experimental studies and approximate analyses the following conclusions can be reached:

- 1) The brittle-coating method provides whole field information of the principal directions and approximate magnitudes of principal stresses. Obviously, the direction in which reinforcing bars should be placed can be found from this method.
- 2) Results obtained from electrical strain gages give good accuracy and can be used for evaluating the approximate numerical methods.
- 3) Eccentricity due to one-sided reinforced opening causes a reduction in efficiency of reinforcement which could be improved by reinforcement on both sides of the web.
- 4) Numerical methods require a computer program. This is not expensive but it is complicated compared to other methods.
- 5) If the reinforcement is not too close to the corner and can provide enough space for welding, the stress concentration at the corner can be reduced.
- 6) It is recommended that the best way of locating the reinforcement should be found by using the idea of structural optimization to write a computer program with enough iterations to obtain the best angle for placement of the reinforcement.

APPENDIX I

Computation of Normal Stress Distributions by Winkler's Curved Beam

Theory

Based on Winkler's Theory, the normal stresses at the corners of the opening were calculated as following:

(i) Unreinforced Opening

a) For section A-A under loading Case I, the freebody diagram is shown in Fig. A.

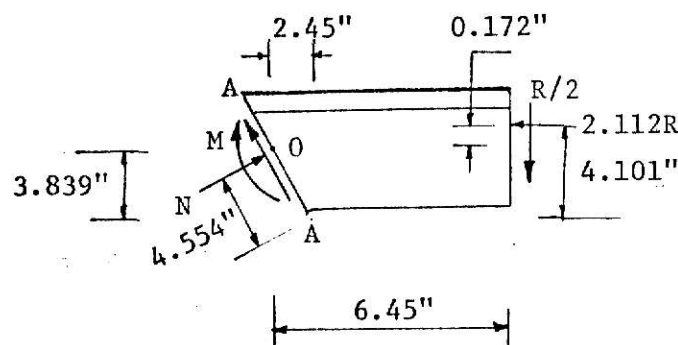


Fig. A Freebody Diagram for Loading Case I.

M , N are the moment and normal force, they were calculated by statical equilibrium conditions.

$$M = -2.862 R ,$$

and $N = -1.558 R .$

Where R is the reaction force at the supports of the beam.

The effective width of flange can be calculated according to Bleich's analysis as adopted by Seely and Smith (20).

$$b' = \alpha b \quad (1)$$

where b' = reduced or effective projecting width of flange (on each side)

b = projecting width of the actual flange (on each side)

α = a reduction factor in Bleich's solution

b^2/rt was found equal to 2.91, from Table 6, PP. 162, (20), α can be obtained to be 0.421. Thus, b' was calculated as follows:

$$b' = 0.421 \times \left(\frac{7.073 - 0.38}{2} \right) = 1.409'' .$$

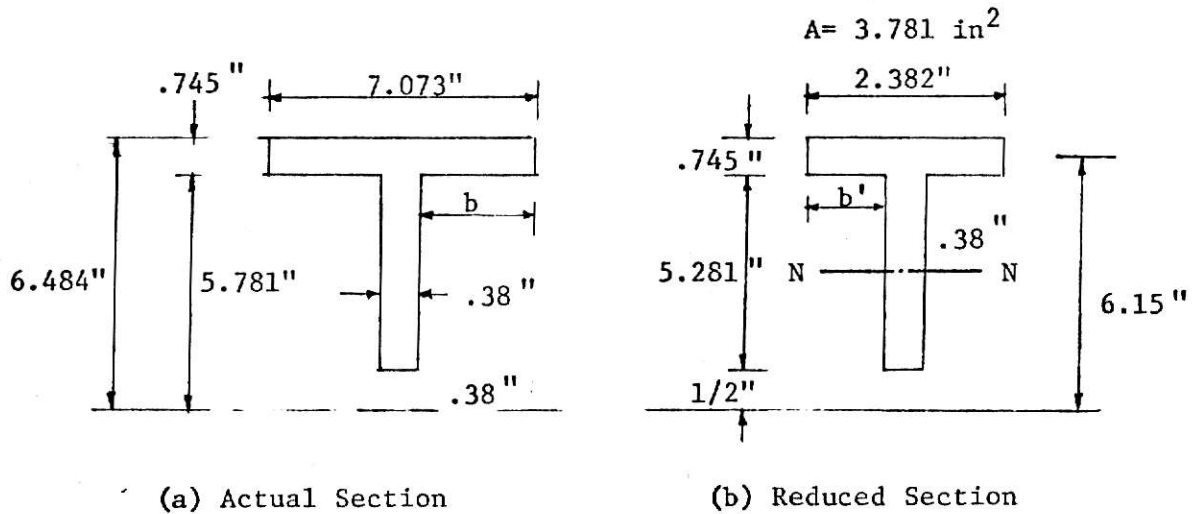


Fig. B Dimensions of Section A-A

Reduction of the flange width due to its direction not normal to section A-A is given by

$$b'' = 1.409 \times (\cos \theta)^2 = 1.001'' .$$

Total width of flange was found to be 2.382". This leads to the reduced dimensions as shown in Fig. Bb.

Using Winkler's curved beam theory, the parameter m can be expressed as following:

$$m = \frac{\bar{r}}{A} (b_1 \ln \frac{r_1}{r_2} + b_2 \ln \frac{r_2}{r_1}) - 1 \quad (2)$$

where A is the total area of the section.

\bar{r} , b_1 , b_2 , r_1 , r_1 and r_2 for section A-A were shown in Fig. C.

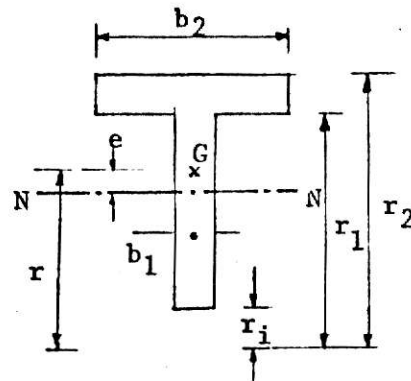
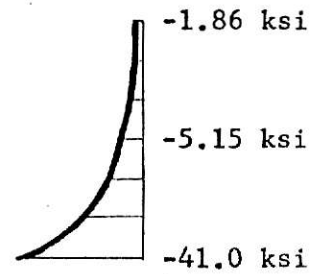


Fig. C Typical Section



(Case I)

Fig. D Normal Stress Curve
for Section A-A

$$m = \frac{4.554}{3.781} (.38 \ln \frac{5.781}{.5} + 2.382 \ln \frac{6.484}{5.781}) - 1 = .4441$$

The distance between the neutral axis and the centroidal axis was calculated.

$$e = \bar{r} \frac{m}{m+1} = 4.554 \frac{.4441}{1.4441} = 1.4005''.$$

From

$$\sigma(y) = \frac{N}{A} + \frac{M(y - e)}{A e (r - y)}, \quad (3)$$

Substituting N, M, A, e and \bar{r} into eqns. (3), $\sigma(y)$ can be calculated by

$$\sigma(y) = (-0.412 - 0.541 \times \frac{(y - 1.4)}{(4.554 - y)}) R \quad (4)$$

The normal stress calculated from eqns. (4) was shown in Fig. D.

b) For section B-B under loading Case II, the freebody diagram was shown Fig. E.

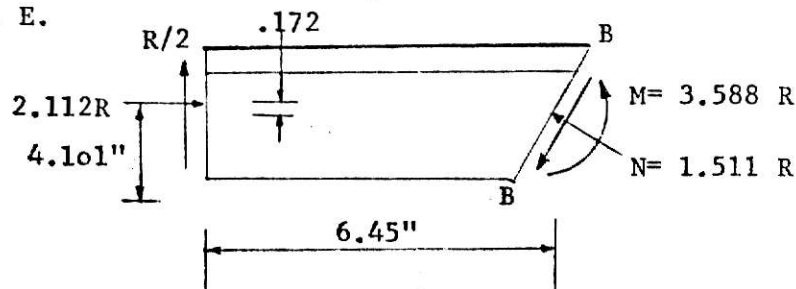


Fig. E Freebody Diagram for Section B-B

Note that the section property constants of section B-B are the same as those of section A-A. Therefore

$$\sigma(y) = (-0.340 + 0.678 \times \frac{(y - 1.4)}{(4.554 - y)}) R \quad (5)$$

Using eqns. (5), the normal stress curve can be calculated, as shown in Fig. F.

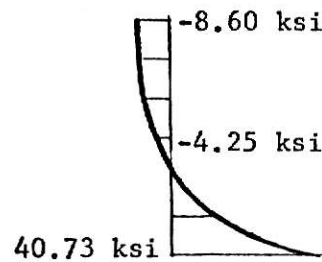


Fig. F Normal Stress Curve for Section B-B
(Loading Case II)

(ii) For Reinforced Opening

a) For section D-D under Loading Case I, the freebody diagram was shown in Fig. G, with M , N and \bar{r} as indicated.

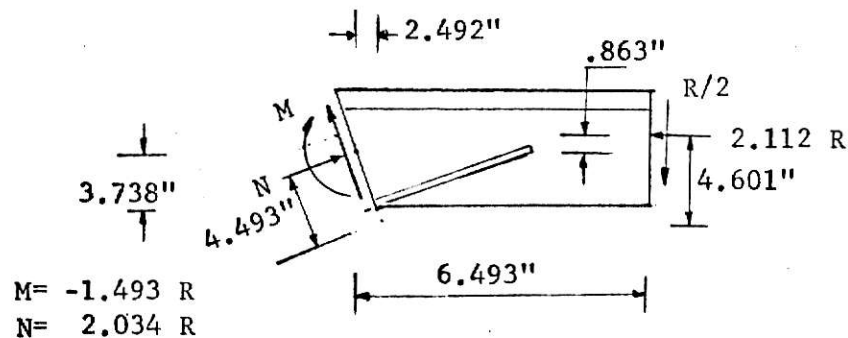


Fig. G. A Freebody Diagram for Section D-D

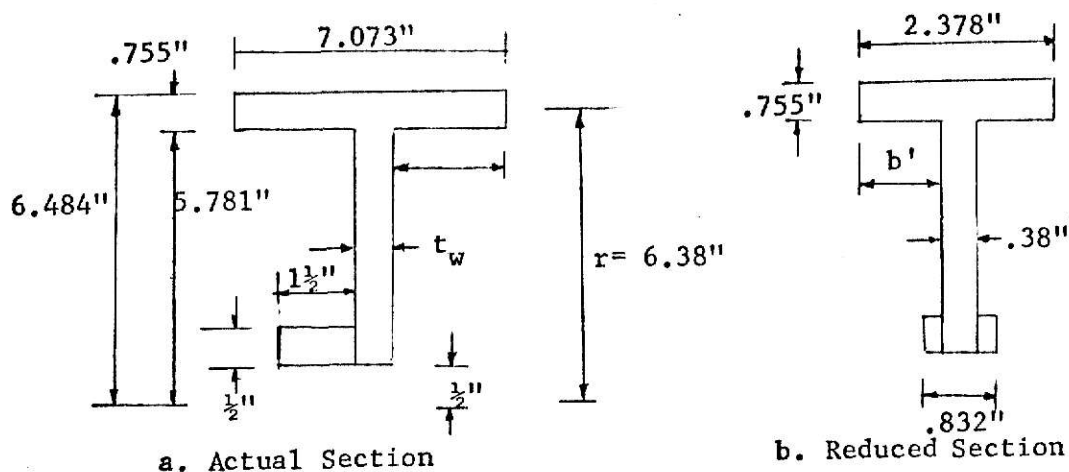


Fig. H Dimensions of Section D-D

With the same calculation as for section A-A, the values of the parameters for finding effective width of flange and reinforcing bars were computed and listed in Table A.

Table A. Computation of Effective Width and Section Properties

	b	r	t	b^2/rt	α	αb	$\alpha b \cos^2 \theta = b'$	$2b' + t_w$
Flange	3.347	6.380	0.628	2.796	0.431	1.443	0.999	2.378
Reinforcements	1.5	0.75	0.5	6.0	0.301	0.452	0.452	0.832
$A=4.1 \text{ in}^2$, $\bar{r}=4.493''$, $m=0.688$, $e=1.831''$								

The equation for calculating normal stress for section A-A can be expressed as follows:

$$\sigma(y) = (-0.496 - 0.191 \frac{(y - 1.831)}{(4.493 - y)}) R \quad (6)$$

The normal stress curve calculated by eqn. (6) with $R=12.5^k$ was shown in Fig. K

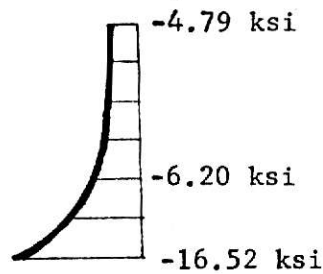


Fig. K Normal Stress Curve for Section D-D
(Loading Case I)

b) For section C-C under Loading Case II, the freebody diagram was shown in Fig. L, with M, N and \bar{r} indicated.

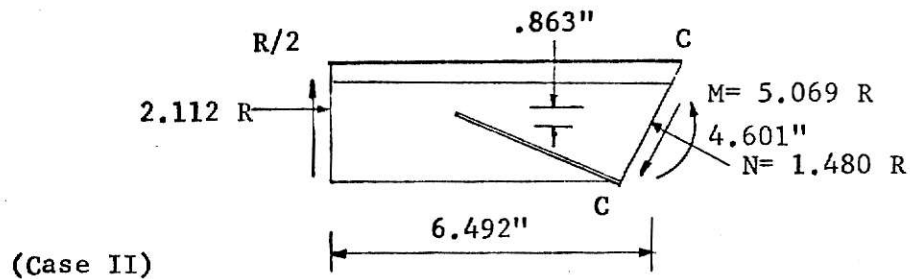


Fig. L Freebody Diagram for Section C-C

Using the property constants listed in Table A, and M, N and \bar{r} shown in Fig. L, the normal stress function was obtained

$$\sigma(y) = \left(-.361 + .675 \frac{y - 1.831}{4.493 - y} \right) R \quad (7)$$

Results calculated from eqn. (7) was shown in Fig. Q

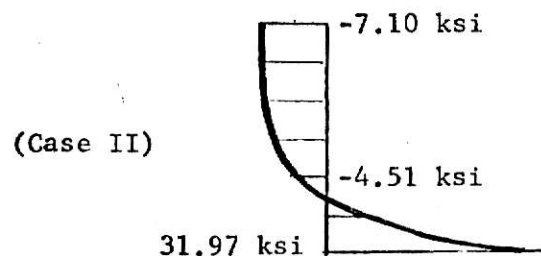


Fig. Q Normal Stress Curves for Section C-C

APPENDIX II

Computation of Stress Distribution Based on Stress-Coating Method

(1) Temperature and humidity during spray and each loading level were recorded. All the calibration bars used experienced the same atmospheric conditions. At each loading level one calibration bar was used to experience the same loading-time history as the beam tested. The calibrated results were used to predict the coating threshold strain.

TABLE B A RECORD OF BRITTLE COATING TEST

Load (Kips)	Date	Time	Temp (°F)	R.H. (%)	Bar No.	Load Duration (hrs.)	Thick- ness (in)	Threshold Strain($\mu\epsilon$)
0	8/5/75	11:30 AM	80	65	B1		0.010	400
15	8/5/75	12:00 PM	80	65				
0	8/5/75	10:00 PM	83	65	B2	10	0.013	420
25	8/5/75	11:30 PM	83	65				
0	8/6/75	9:30 AM	81	62	B3	10	0.016	340
35	8/6/75	10:40 AM	81	62				
0	8/6/75	8:40 PM	80	55	B4	10	0.015	340
45	8/6/75	10:00 PM	80	55				
0	8/7/75	9:00 AM	79	65	B5	11	0.015	420
55	8/7/75	12:45 PM	80	62				
0	8/7/75	9:30 PM	82	59	B6	9	0.014	510

(ii) Corrections due to temperature and humidity

According to manufacture's bulletin, TL-201, the threshold strain increases approximately $5 \mu\epsilon$ per percent R.H. increase for small changes in R.H. and decreases approximately $35 \mu\epsilon$ per degree of Fahrenheit for small changes in temperature.

Table C shows the calculation of corrections due to temperature and R.H. and the approximate threshold strain at reference temperature and humidity (80°F and 65% R.H.).

Table C Threshold Strain Correction Due to Temperature and R.H.

	Threshold Strain	Correction		Threshold Strain D 80°F, 65% R.H.	Corrected Threshold Strain
	$\mu\epsilon$	Temp	R.H.	$\mu\epsilon$	$\mu\epsilon$
B2	420	-105	0	315	518
B3	420	- 35	15	400	433
B4	340	0	50	390	363
B5	420	35	0	455	378
B6	510	- 70	30	470	453

Average= 406

(iii) Correction due to Loading Velocity

$$\begin{aligned}
 \epsilon_t^{**} &= 1 + 0.05 (\log_{10} t)^2 \epsilon_t^* \\
 &= 1 + 0.05 (\log 4)^2 \\
 &= 1.018 \epsilon_t^* \text{ (Correction due to the time of releasing load)} \\
 &= 1.018 \times 406 = 413 \mu\epsilon
 \end{aligned}$$

(iv) Calculation of Apparent Stress at 25 Kips

The normal stresses along the critical sections were calculated and listed in Table D.

Table D Computation of Apparent Stress by Brittle-Coating Method

Load (Kips)	ϵ	$\sigma \approx E\epsilon$ (ksi)	σ_{25} (ksi)	d (in.)	d' (in.)
15	518	15.0	25.0	1/8	
25	433	12.5	12.5	1/2	1/4
35	363	10.5	7.5	1-3/4	1
45	378	11.0	6.1	4	3
55	453	13.1			5

Note: Unit of strain is in micro-inch/inch.

(V) Normal Stress Curves

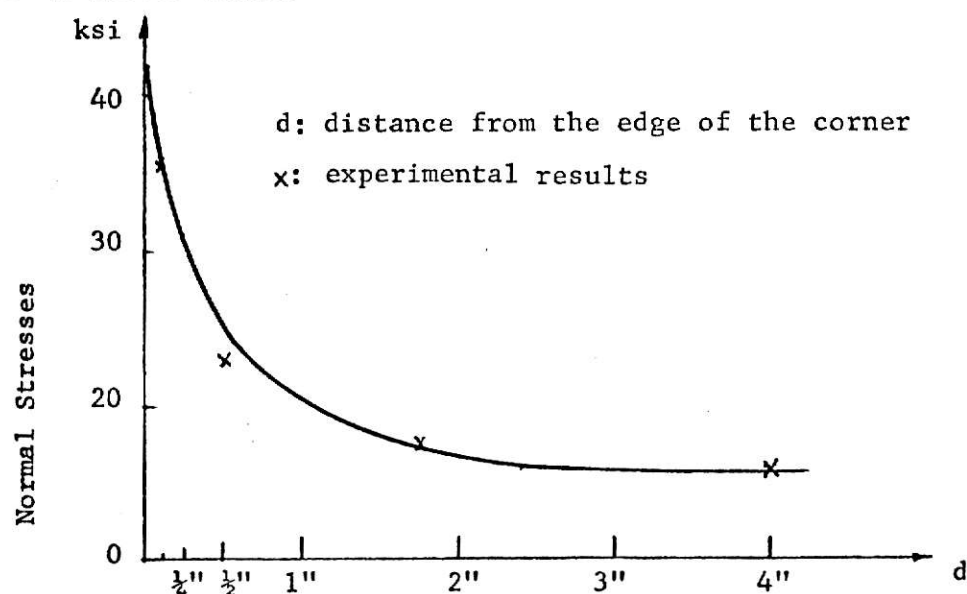


Fig. R Normal Stress Curves for Unreinforced Corner by Brittle-Coating Method

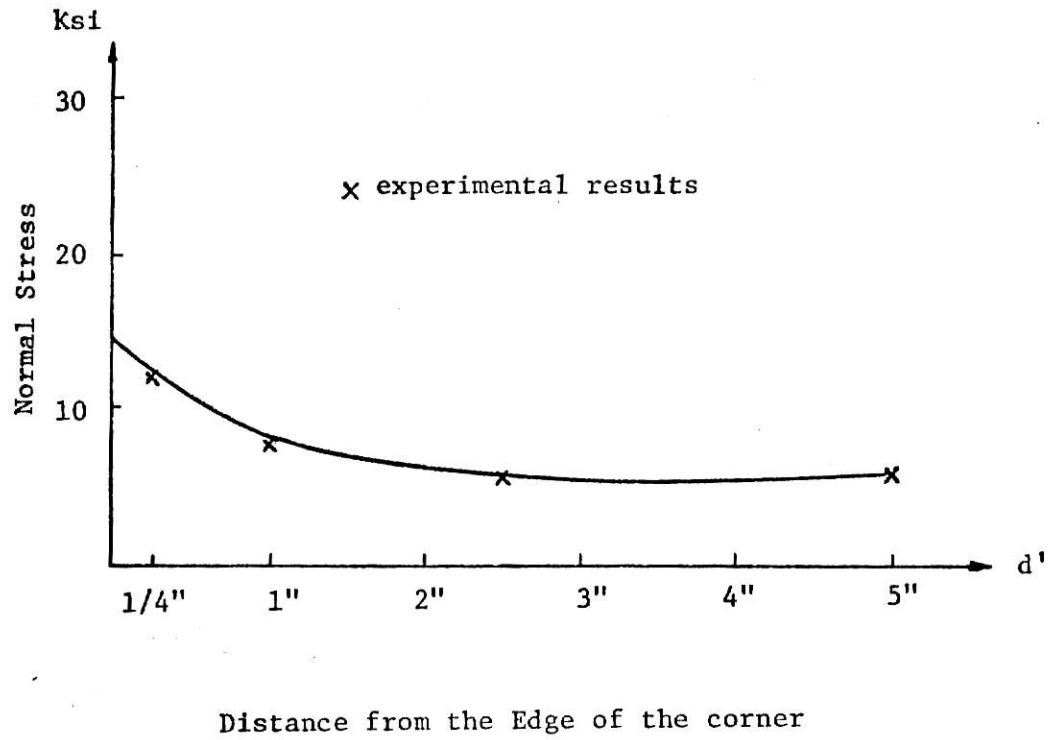


Fig. S Normal Stress Curve for Reinforced Corner
by Brittle-Coating Method

REFERENCES

1. Muskhelishvili, N. I., "Some Basic Problems of the Mathematical Theory of Elasticity", 2nd Edition, P. Noordhoff Ltd., 1963.
2. Heller, S. R., Jr., J. S. Brock , and R. Bart , "The Stresses around a Rectangular Opening with Rounded Corner in a Uniformly Loaded Plate", Proc. 3rd. National Contress of Applied Mechanics, 1958.
3. Heller, S. R., Jr., J. S. Brock , and R. Bart , "The Stresses around a Rectangular Opening with Rounded Corners in a Beam Subjected to Bending and Shear", Proc. 4th National Congress of Applied Mechanics, 1962.
4. Bower, J. E., "Elastic Stresses around Holes in Wide-Flange Beams", Journal of the Structural Division, ASCE, Vol. 92, No. ST5, April, 1966.
5. Bower, J. E., "Experimental Stresses in Wide Flange Beams with Holes", Journal of Structural Division, ASCE, Vol. 92, No. ST5, Oct., 1966.
6. Arora, J. S., "Experimental Stress Analysis of an I-Beam with a Rectangular Web Cut-Out", a Master's Thesis, KSU, 1967.
7. Cheng, K. S., "Experimental Study of Beams with Web Openings", Master's Thesis, KSU, 1969.
8. Cooper, P. B. and R. R. Snell, "Tests on Beams with Reinforced Web Openings", Journal of Structural Division, ASCE, Vol. 98, No. ST3, March 1972.
9. Hu, K. K. and H. K. Woo, "Stress around Web Openings in Elastic Beam and the Design of Reinforcing to Reduce Them", Technical

- Reports, Experimental Station, KSU, April, 1974.
10. Wang, T. M., R. R. Snell and P. B. Cooper, "Strength of Beams with Eccentric Reinforced Holes", Proc. ASCE, Journal of Structural Division, Vol. 101, No. ST9, Sept., 1975.
 11. Redwood, R. G. and J. O. McCutcheon, "Wide-Flange Beams Containing Large Unreinforced Web Openings", Structural Mechanics Series, No. 2, McGill University, Montreal, Canada, Sept., 1967.
 12. Dally, J. W. and W. F. Riley, "Experimental Stress Analysis", McGraw-Hill, Inc., 1965.
 13. "Instructions for the Selection and Use of Tens-Lac Brittle Lacquers and Undercoatings", Bulletin TL-201 Photolastic Inc.
 14. Chan, P. W. and R. G. Redwood, "Stresses in Beam with Eccentric Holes", Journal of the Structure Division, ASCE, Vol. 100, No. ST1, Jan. 1972.
 15. Den Hartog, J. P., "Advanced Strength of Material", PP. 223-226, McGraw-Hill Book Co., Inc., New York, 1951.
 16. Hsu, Y. I., "Plate Bending Finite Element Analysis of Beams with Web Openings", a Master's Report, KSU, 1972, PP. 50-65.
 17. Lee, H. H., "Plate Bending Finite Element Analysis of Beams with Web Openings", a Master's Report, KSU, 1972, PP. 50-65.
 18. Timoshenko, S., "Strength of Material", Part I, PP. 362-375, 3rd edition, D. Van Nostrand Co., Inc., N. Y. 1955.
 19. Timoshenko, S., and J. N. Goodier, "Theory of Elasticity", PP. 73-76, McGraw Hill Book Co., N. Y. 1951.

ACKNOWLEDGEMENTS

The author wishes to express his most sincere appreciation and gratitude to his advisor, Dr. K. K. Hu, for his valuable instructions in preparing this thesis and constant encouragements to his study.

Thanks are also due to Prof. Frank J. McCormick for his guidances and suggestions in experimental programs, and to Dr. Stuart E. Swartz and Dr. Hugh S. Walker for their serving in advisory committee.

He would like also to thank Dr. Robert R. Snell and Dr. Peter B. Cooper for providing the experimental materials.

EXPERIMENTAL AND NUMERICAL ANALYSIS
OF STRESSES AROUND UNREINFORCED
AND REINFORCED WEB OPENINGS

by

JAMES CHEN-MING HUANG

DIPLOMA, TAIPEI INSTITUTE OF TECHNOLOGY, 1969

AN ABSTRACT OF A MASTER'S THESIS
submitted in partial fulfillment of the
requirements for the degree

MASTER OF SCIENCE

Department of Civil Engineering

KANSAS STATE UNIVERSITY

Manhattan, Kansas

1976

ABSTRACT

This study presents the results of experimental analysis of an I-beam with web opening by means of brittle coatings and electrical resistance strain gages. These results were compared with numerical calculations.

Brittle-coating results indicated the directions and locations of critical sections where the electrical resistance strain gages were used.

Least work method was based on stress distribution function to minimize local strain energy density function and on the statically indeterminate forces to minimize the total potential energy.

Vierendeel truss method was used for finding the internal resultant forces. The stress distributions over the section were calculated using curved beam theory.